

# Early intervention with 3BNC117 and romidepsin at antiretroviral treatment initiation in people with HIV-1: a phase 1b/2a, randomized trial

Received: 15 March 2022

Accepted: 22 August 2022

Published online: 17 October 2022

 Check for updates

A list of authors and their affiliations appears at the end of the paper

Attempts to reduce the human immunodeficiency virus type 1 (HIV-1) reservoir and induce antiretroviral therapy (ART)-free virologic control have largely been unsuccessful. In this phase 1b/2a, open-label, randomized controlled trial using a four-group factorial design, we investigated whether early intervention in newly diagnosed people with HIV-1 with a monoclonal anti-HIV-1 antibody with a CD4-binding site, 3BNC117, followed by a histone deacetylase inhibitor, romidepsin, shortly after ART initiation altered the course of HIV-1 infection (NCT03041012). The trial was undertaken in five hospitals in Denmark and two hospitals in the United Kingdom. The coprimary endpoints were analysis of initial virus decay kinetics and changes in the frequency of CD4<sup>+</sup> T cells containing intact HIV-1 provirus from baseline to day 365. Secondary endpoints included changes in the frequency of infected CD4<sup>+</sup> T cells and virus-specific CD8<sup>+</sup> T cell immunity from baseline to day 365, pre-ART plasma HIV-1 3BNC117 sensitivity, safety and tolerability, and time to loss of virologic control during a 12-week analytical ART interruption that started at day 400. In 55 newly diagnosed people (5 females and 50 males) with HIV-1 who received random allocation treatment, we found that early 3BNC117 treatment with or without romidepsin enhanced plasma HIV-1 RNA decay rates compared to ART only. Furthermore, 3BNC117 treatment accelerated clearance of infected cells compared to ART only. All groups had significant reductions in the frequency of CD4<sup>+</sup> T cells containing intact HIV-1 provirus. At day 365, early 3BNC117 + romidepsin was associated with enhanced HIV-1 Gag-specific CD8<sup>+</sup> T cell immunity compared to ART only. The observed virological and immunological effects of 3BNC117 were most pronounced in individuals whose pre-ART plasma HIV-1 envelope sequences were antibody sensitive. The results were not disaggregated by sex. Adverse events were mild to moderate and similar between the groups. During a 12-week analytical ART interruption among 20 participants, 3BNC117-treated individuals harboring

sensitive viruses were significantly more likely to maintain ART-free virologic control than other participants. We conclude that 3BNC117 at ART initiation enhanced elimination of plasma viruses and infected cells, enhanced HIV-1-specific CD8<sup>+</sup> immunity and was associated with sustained ART-free virologic control among persons with 3BNC117-sensitive virus. These findings strongly support interventions administered at the time of ART initiation as a strategy to limit long-term HIV-1 persistence.

In the human immunodeficiency virus type 1 (HIV-1) infection, integration of the viral genome into the DNA of immune cells establishes a long-lived HIV-1 reservoir. Cohort studies have shown that the integrated proviruses present during long-term antiretroviral therapy (ART) primarily consist of viruses that were circulating in plasma the year before ART initiation<sup>1–5</sup>. Due to the persistence of the HIV-1 reservoir, viral replication quickly resumes following ART interruption, leading to rebound of viremia within weeks in almost all individuals regardless of treatment duration<sup>6–10</sup>. Thus, life-long ART is currently necessary to suppress viral replication and prevent disease progression.

Until now, HIV-1 cure-related trials have almost exclusively focused on persons who have been on long-term suppressive ART. The ‘kick and kill’ HIV-1 cure strategy aims at reducing or eliminating the viral reservoir by activating HIV-1 transcription and thus enabling the immune-mediated killing of latently infected cells. Clinical trials testing latency-reversing agents (LRAs) such as histone deacetylase inhibitors (HDACi) have shown that viral transcription in latently infected cells can be (re)activated, but thus far no clinically meaningful reduction in viral reservoir size has been observed in humans<sup>6,8,10–18</sup>. Romidepsin (RMD) is one of the HDACi that in some clinical trials has been shown to induce HIV-1 expression in infected CD4<sup>+</sup> T cells<sup>19–21</sup>. To boost HIV-1-specific immunity and enhance immune-mediated killing following latency reversal<sup>22</sup>, therapeutic HIV-1 vaccines have been tested in combination with RMD. Two studies found that this combination strategy led to a modest decline in the HIV-1 reservoir, but no significant immune-mediated control of plasma viremia was observed during a subsequent analytical treatment interruption (ATI)<sup>9,23</sup>. A third and larger randomized study found no impact on the size of the viral reservoir when combining therapeutic HIV-1 vaccines with vorinostat, another HDACi<sup>24</sup>.

A different potential strategy for enhancing HIV-1-specific immunity is through the administration of broadly neutralizing anti-HIV-1 antibodies (bNAbs) recognizing the HIV-1 envelope protein, gp120. In addition to direct neutralization of cell-free virus, bNAbs can also engage the immune system through their Fc domains and form antibody–antigen immune complexes<sup>25–27</sup>. These antibody–antigen immune complexes have been proposed to mediate a vaccinal effect that may lead to improved HIV-1-specific cellular immunity<sup>28–32</sup>. However, in long-term ART-treated individuals, levels of cell-free virus or HIV-1 envelope expression on infected cells may be too low to adequately engage Fc-mediated effector functions, and in two recent trials in ART-suppressed individuals, the bNAbs 3BNC117 and VRC07-523LS, each in combination with an HDACi, failed to reduce the intact HIV-1 reservoir size<sup>10,33</sup>.

Interestingly, early treatment with bNAbs but not ART in simian/HIV (SHIV)<sub>AD8-E0</sub>-infected nonhuman primates induced long-lasting HIV-1-specific immunity and durable immune-mediated control proposed to be at least in part due to SHIV-specific CD8<sup>+</sup> T cells after the levels of bNAbs had waned<sup>31,34</sup>. In addition, a mathematical modeling study suggested that latency reversal at ART initiation may have a far greater impact on infected cells than latency reversal after years of ART due to ongoing immune activation<sup>20,34–37</sup>.

Collectively, the lack of success of HIV-1 cure-related trials in long-term ART-treated individuals combined with the potential window

of opportunity in newly diagnosed ART-naive individuals as outlined above led us to hypothesize that bNAbs with or without an LRA administered during ART initiation could potentially enhance the elimination of infected cells, reduce the size of the HIV-1 reservoir and improve HIV-1-specific T cell immunity. We conducted an investigator-initiated phase 1b/2a, open-label, multicenter, randomized controlled trial among individuals initiating ART to determine the safety and effects of 3BNC117 and/or RMD on decay of plasma viremia, dynamics of active HIV-1-infected cells, size of the HIV-1 reservoir, HIV-1-specific T cell immunity and duration of virologic control during a subsequent 12-week ATI (Fig. 1a).

## Results

### Participants and follow-up

Eligible individuals were recruited from 16 January 2017 to 3 March 2020, and the last follow-up visit occurred on 17 July 2021. Of the total 60 participants enrolled in the study, 55 received the random allocation treatment (Fig. 1b and Extended Data Fig. 1). One participant was not randomized due to newly imposed national restrictions on non-coronavirus disease 2019 (COVID-19) research. Three other participants withdrew consent for personal reasons and did not receive the allocated treatment (one in the ART + RMD group and two in the ART + 3BNC117 + RMD group). One participant in the ART + 3BNC117 group was taken out of the study due to hospital admission with gram-negative bacteremia before receiving the first dose of 3BNC117. Of the remaining 55 (92%) participants, 15 were randomly allocated to the ART-only group, 14 to the ART + 3BNC117 group, 12 to the ART + RMD group and 14 to the ART + 3BNC117 + RMD group. Two participants missed one of the three scheduled RMD infusions: one due to low neutrophil count (ART + RMD group) and one due to influenza A infection (ART + 3BNC117 + RMD group). Three participants were lost to follow-up before day 365, of whom two moved out of the study area (one in the ART + 3BNC117 group and one in the ART + RMD group), and one participant had a relapse of psychiatric illness (ART + RMD group). The first administration of the two study drugs was spaced 7 to 10 days after ART initiation to distinguish the potential relatedness of adverse events to ART and the study drugs.

The four groups were overall well balanced (Table 1 and Extended Data Table 1). Study participants were mainly (81%) Caucasian males and the median age was 36 years (interquartile range (IQR), 28–47 years). The proportion of participants with recent HIV-1 infection (<6 months from date of infection to study enrollment) ranged from 27% in the ART + 3BNC117 group to 67% in the ART-only group. Self-reported time of infection was confirmed by antibody-based recency testing (Extended Data Fig. 2). At baseline, the median CD4<sup>+</sup> T cell count was 503 cells per mm<sup>3</sup> (range: 203–1,497) and the median plasma HIV-1 RNA level was 49,400 copies per ml (range: 730–24,000,000) for the total study population (Extended Data Table 1). Approximately half of the individuals (49%) had HIV-1 subtype B infection, whereas the rest of the participants had a broad range of other HIV-1 subtypes and recombinant forms (Extended Data Table 1). Human leukocyte antigen (HLA) class I alleles known to be associated with rapid HIV-1 progression (that is, HLA-B\*07 and HLA-B\*35) and elite control (that is, HLA-B\*27,

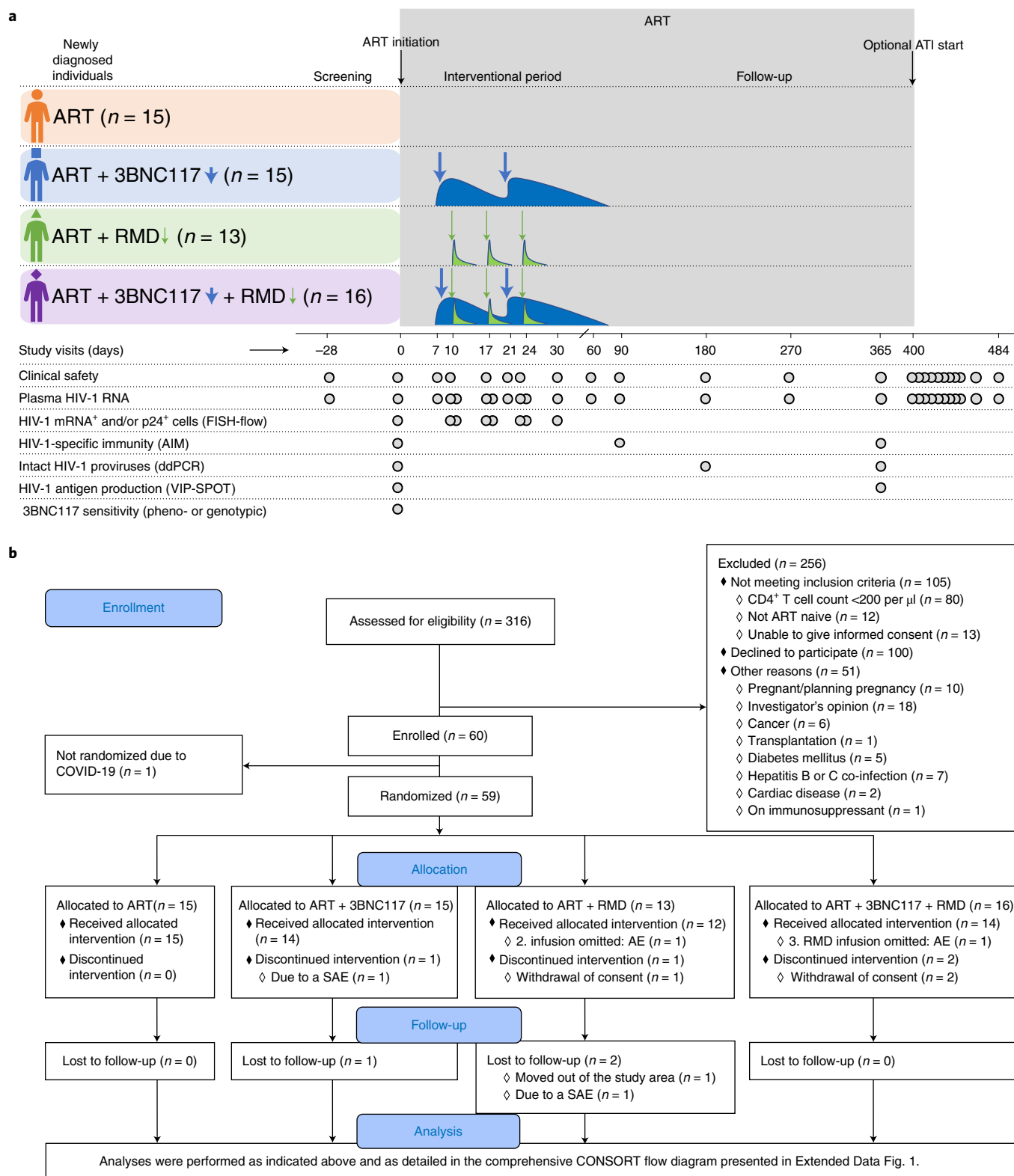


**Fig. 1 | Trial design and participant flow diagram. a, b,** The eCLEAR trial design (a) and abbreviated CONSORT flow diagram (b). The analysis section is presented in full in Extended Data Fig. 1. SAE, severe adverse event.

HLA-B\*57 and HLA-B\*58) were represented in 44% of the participants across all four groups (Extended Data Table 1). Post hoc bNAbs sensitivity testing of baseline plasma samples revealed that 8 of 15 (53%) participants in the ART + 3BNC117 group and 10 of 16 (63%) participants in the ART + 3BNC117 + RMD group had 3BNC117-sensitive plasma viruses at baseline (Fig. 2a). Notably, the individuals (n = 18) harboring pre-ART

3BNC117-sensitive viruses were comparable to the individuals (n = 13) harboring pre-ART 3BNC117-resistant viruses (Supplementary Table 1).

### Decay rates of plasma HIV-1 RNA after ART initiation

Individuals with the lowest pre-ART plasma HIV-1 RNA levels were generally suppressed within 7–17 days after ART initiation, but not every

**Table 1 | Baseline characteristics of the study population**

	ART (n=15)	ART + 3BNC117 (n=15)	ART + RMD (n=13)	ART + 3BNC117+RMD (n=16)
Age (years)	33 (25–58)	41 (25–69)	32 (18–68)	37 (22–57)
Female sex	4 (27)	0 (0)	1 (8)	0 (0)
Race				
Asian	1 (7)	1 (7)	1 (8)	2 (13)
Black or African European	2 (13)	0 (0)	1 (8)	0 (0)
White or Caucasian	12 (80)	13 (86)	9 (69)	14 (88)
Other	0 (0)	1 (7)	2 (15)	0 (0)
Time from infection to study enrollment <sup>a</sup>				
Recent (<6 months)	10 (67)	4 (27)	5 (38)	9 (56)
Long-term (>6 months)	5 (33)	9 (60)	7 (54)	6 (38)
Unknown	0 (0)	2 (13)	1 (8)	1 (6)
CD4 <sup>+</sup> T cell count (cells per mm <sup>3</sup> )	560 (252–1,497)	506 (218–984)	391 (286–1,333)	531 (203–1,098)
HIV-1 RNA level (copies per ml)	39,207 (820–3,240,000)	56,800 (740–24,000,000)	49,400 (3,800–1,900,000)	50,000 (730–4,180,000)
HIV-1 subtype <sup>b</sup>				
B	7 (47)	7 (47)	6 (46)	8 (50)
Non-B	8 (53)	8 (53)	7 (54)	8 (50)
HLA class I alleles <sup>b</sup>				
Risk: HLA-B*07, HLA-B*35	6 (40)	4 (27)	4 (31)	2 (13)
Protective: HLA-B*27, HLA-B*57, HLA-B*58	3 (20)	1 (7)	2 (15)	5 (31)

Data are median (range) or *n* (%). <sup>a</sup>Time from infection to study enrollment was self-reported. <sup>b</sup>Individual HIV-1 subtypes and HLA class I alleles can be found in Extended Data Table 1.

individual had sustained viral suppression after 365 days of ART (Fig. 2b). To compare plasma viral load kinetics after ART initiation among the four groups, we split the decay rate of plasma HIV-1 RNA levels into three phases (Fig. 2c,d). During the first phase from the day of ART initiation to day 10, the median plasma HIV-1 RNA decay rates were comparable between the four groups. From days 10–24 of ART, the daily decay rate in median HIV-1 RNA was significantly faster for the ART + RMD + 3BNC117 group with a decrease of 16.9% (95% confidence interval (CI), –27.3%, –4.93%) compared to 10.0% (95% CI, –14.9%, –4.86%) in the ART-only group ( $P = 0.048$ ). The daily decay rate was also significantly faster for the ART + RMD group (median, 18.5%; 95% CI, –29.0%, –6.51%;  $P = 0.017$ ). From day 24 to day 90 of ART, the decay rates in median HIV-1 RNA levels were comparable between the groups. When both groups receiving 3BNC117 were analyzed according to 3BNC117 sensitivity, the daily percentage decay rates in median HIV-1 RNA were significantly faster among individuals with 3BNC117-sensitive viruses in both the ART + 3BNC117 ( $P = 0.045$ ) and ART + RMD + 3BNC117 ( $P = 0.042$ ) groups compared to the ART-only group from day 10 to 24 of ART (Fig. 2d). There was no significant difference in decay rates among individuals with 3BNC117-resistant viruses compared to the ART group (Fig. 2d). We conclude that 3BNC117 and RMD alone or in combination at ART initiation led to faster second-phase plasma HIV-1 RNA decay than ART alone and that the effect of 3BNC117 was dependent on pre-ART plasma virus sensitivity to the bNAb.

### Impact of 3BNC117 on active HIV-1-infected cells

We next sought to determine whether the faster decay in plasma viremia among 3BNC117-treated individuals was accompanied by enhanced elimination of infected cells. To this end, we used a single-cell RNA fluorescence in situ hybridization-flow cytometry (FISH-flow) assay to quantify HIV-1 transcriptionally and/or translationally active cells during the first 30 days of ART<sup>38</sup>. At baseline, the median number of CD3<sup>+</sup> CD8<sup>+</sup> T cells expressing HIV-1 mRNA, Gag p24 protein or

both per 10<sup>6</sup> cells in our study population was 180 (IQR, 150–230), 89 (IQR, 41–100) and 89 (IQR, 41–100), respectively. These measures of infected cells correlated with baseline plasma HIV-1 RNA, CD4<sup>+</sup> T cell count and CD4/CD8 ratio (Supplementary Fig. 1a). There was no significant change in the number of CD3<sup>+</sup> CD8<sup>+</sup> T cells expressing p24 protein over the first 30 days in the ART-only group (Fig. 3a), but a significant decrease in CD3<sup>+</sup> CD8<sup>+</sup> p24<sup>+</sup> cells was observed in two groups: ART + 3BNC117 (median, 167; IQR, 62–359;  $P = 0.027$ ) and ART + RMD (median, 80; IQR, 20–132;  $P = 0.031$ ) during the first 17 days of ART. Similar trends as those described above were observed for CD3<sup>+</sup> CD8<sup>+</sup>-mRNA<sup>+</sup> and CD3<sup>+</sup> CD8<sup>+</sup> mRNA<sup>+</sup> p24<sup>+</sup> T cells (Extended Data Fig. 3).

To determine the immediate impact of the first 3BNC117 infusion (day 7) on HIV-1 transcription and/or translation, we analyzed the changes in infected cells within the first 10 days. Because both the ART-only and ART + RMD groups only received ART during this period, we could combine data from the two groups and compare them to the combined data from the ART + 3BNC117 and ART + 3BNC117 + RMD groups (Fig. 3b). We observed that the first administration of 3BNC117 led to a significant median fold decline in CD3<sup>+</sup> CD8<sup>+</sup> mRNA<sup>+</sup> (0.45; IQR, 0.32–0.84;  $P = 0.0078$ ) and CD3<sup>+</sup> CD8<sup>+</sup> mRNA<sup>+</sup> p24<sup>+</sup> (0.53; IQR, 0.33–0.69;  $P = 0.0020$ ) T cells (Fig. 3c,d). Similar reductions were observed for CD3<sup>+</sup> CD8<sup>+</sup> p24<sup>+</sup> T cells (Fig. 3e;  $P = 0.074$ ), where this decline was most pronounced among individuals with pre-ART 3BNC117-sensitive viruses (0.49; IQR, 0.20–0.97;  $P = 0.027$ ). Individuals who only received ART did not have significant declines in the frequencies of HIV-1-infected cells (Fig. 3c–e). The 3BNC117-mediated decrease in HIV-1-infected cells during the first 10 days of ART was primarily driven by changes in central memory CD3<sup>+</sup> CD8<sup>+</sup> T cells (Extended Data Fig. 4). We next used viral protein spot (VIP-SPOT) to investigate the long-term effects of the interventions on HIV-1 p24<sup>+</sup> cells<sup>39</sup>. The VIP-SPOT data correlated with baseline plasma HIV-1 RNA and the level of intact proviruses (Supplementary Fig. 1b,c). While all four groups had a significant decrease in the median frequency of induced p24<sup>+</sup> CD4<sup>+</sup>

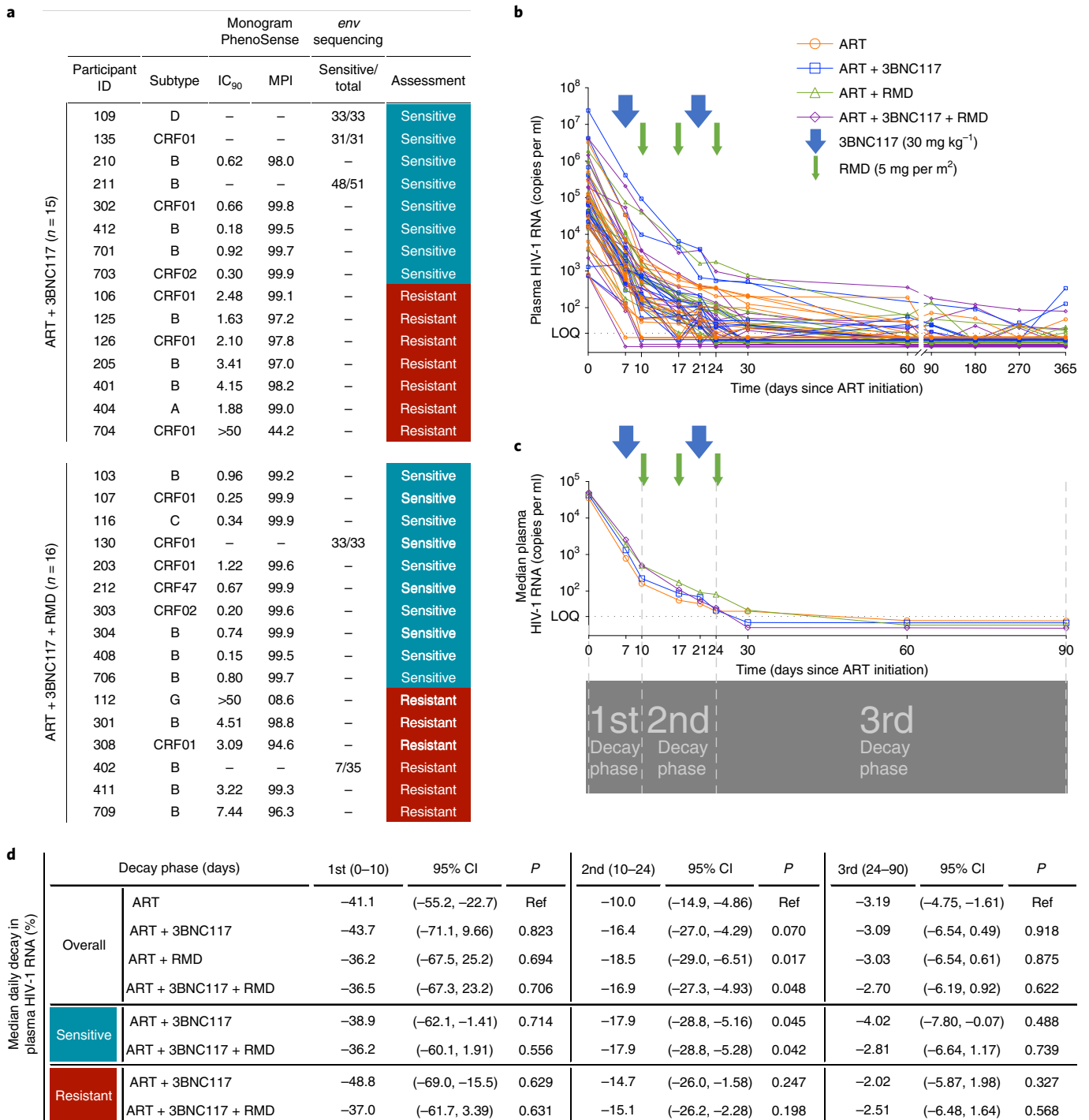


**Fig. 2 | 3BNC117 sensitivity at baseline and median decay of plasma HIV-1 RNA levels following ART initiation.** **a**, 3BNC117 sensitivity at baseline for the ART + 3BNC117 ( $n = 15$ ) and ART + 3BNC117 + RMD ( $n = 16$ ) groups. **b, c**, Individual (**b**) and group (**c**) median decay of plasma HIV-1 RNA levels following ART initiation. The arrows represent 3BNC117 and RMD infusion time points. The horizontal dotted line represents the limit of quantification (LOQ) at 20 copies per ml of the clinical HIV-1 viral load assay. In **c**, the four vertical dashed lines at days 0, 10, 24 and 90 after ART initiation indicate the three plasma HIV-1 RNA decay phases (first phase: 0–10 days; second phase: 10–24 days; and third phase: 24–90 days).

**d**, The percentage decline in median plasma HIV-1 RNA levels per day is presented during the three decay phases following ART initiation in the four randomization groups as well as in groups based on 3BNC117 sensitivity. *P* values were calculated using mixed-effects linear regression models with a random effect for individual participants. We considered a two-sided  $\alpha$  value of less than 0.05 significant with no adjustments made for multiple comparisons. IC<sub>90</sub>, concentration of 3BNC117 required to inhibit viral replication by 90%; MPI, maximum percent inhibition (percent inhibition observed at the highest concentration of 3BNC117 tested); Ref, reference.

T cells from baseline to day 365 (Extended Data Fig. 5a,b), we found that 47% of individuals with 3BNC117-sensitive viruses compared to 33% of individuals with 3BNC117-resistant viruses had no inducible p24<sup>+</sup> CD4<sup>+</sup> T cells at day 365 (Extended Data Fig. 5c). Collectively, these

data demonstrate that 3BNC117 as adjunctive therapy to ART initiation enhanced clearance of HIV-1-infected cells and that this effect was greatest in the central memory compartment—a subset of CD4<sup>+</sup> T cells believed to be important for HIV-1 persistence.

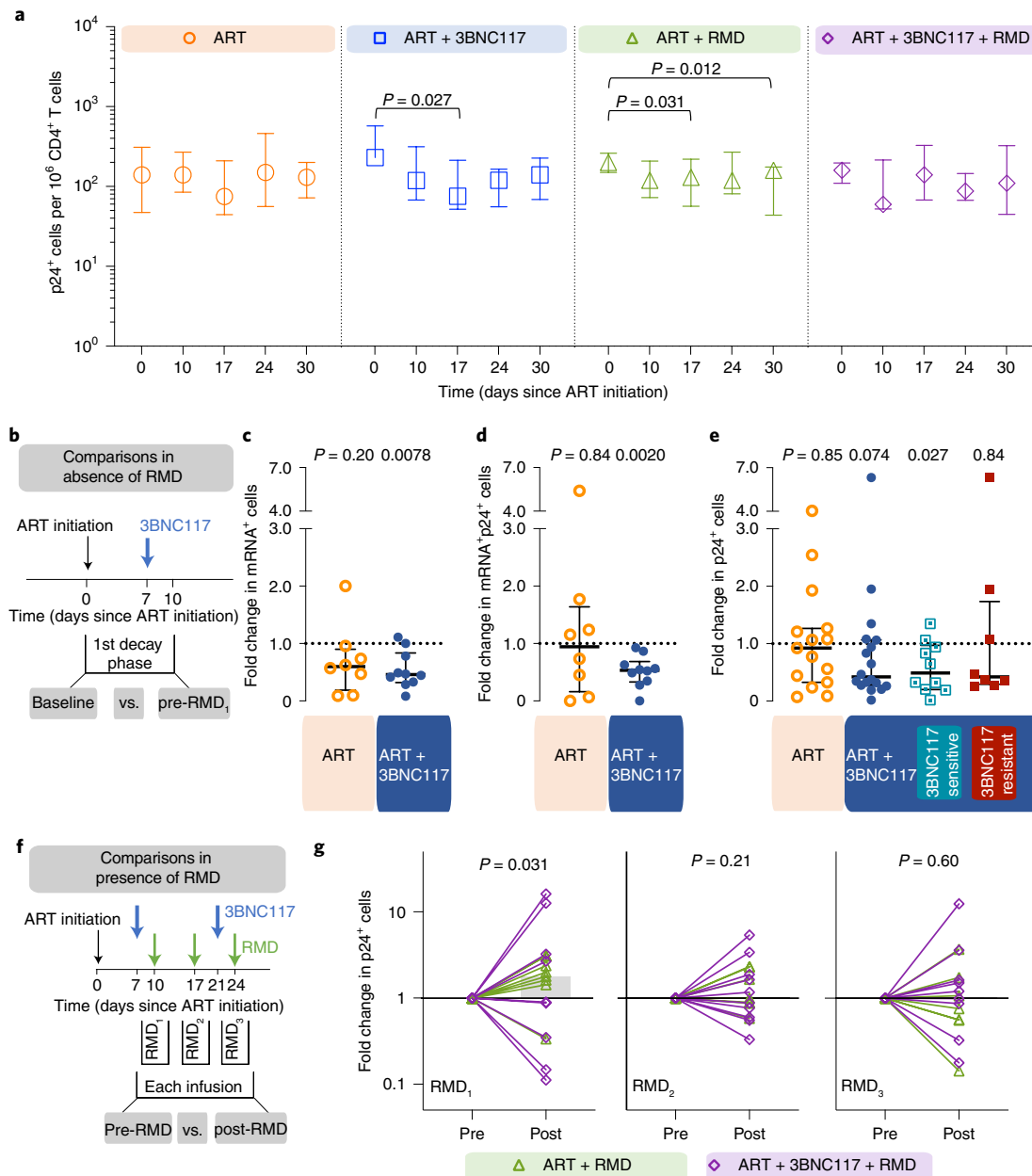


**Fig. 3 | Transcriptionally and/or translationally active HIV-1-infected cells following ART initiation.** **a**, Changes in HIV-1-infected cells during the first 30 days of ART among the four groups shown as median (error bars represent IQR) number of CD3<sup>+</sup> CD8<sup>+</sup> T cells expressing Gag p24 protein per 10<sup>6</sup> CD4<sup>+</sup> T cells (ART, *n* = 7; ART + 3BNC117, *n* = 9; ART + RMD, *n* = 9; ART + 3BNC117 + RMD, *n* = 10). **b–e**, Effect of 3BNC117 on transcriptionally and/or translationally HIV-1-infected cells from baseline to day 10; first decay phase defined in Fig. 2c. **b**, The schematic illustration shows how data were combined from the ART-only and ART + RMD groups (who only received ART during the first 10 days) compared to the two 3BNC117-treated groups. **c–e**, Median (IQR) fold change in CD3<sup>+</sup> CD8<sup>+</sup> T cells expressing HIV-1 mRNA (ART, *n* = 8; ART + 3BNC117, *n* = 10) (**c**), mRNA and p24 (RT, *n* = 8; ART + 3BNC117, *n* = 10) (**d**) or p24 (ART, *n* = 15; ART + 3BNC117, *n* = 18)

(**e**) among the combined ART and ART + 3BNC117 groups, and with the ART + 3BNC117 group categorized according to 3BNC117 sensitivity (sensitive (*n* = 10) versus resistant (*n* = 8)). In **c** and **d**, due to a faulty mRNA probe in the second batch of FISH-flow cytometry analyses, mRNA data were only available for half of the study population. **f**, The schematic illustration shows how we analyzed the pre- to postinfusion effect of RMD on translationally active HIV-1-infected cells. **g**, Individual and overall median fold change (gray column) from pre- to post-RMD infusions (overall median (IQR) for RMD<sub>1</sub>, 1.78 (0.61–3.09), RMD<sub>2</sub>, 1.00 (0.68–2.09), and RMD<sub>3</sub>, 1.03 (0.56–1.70)) in groups ART + RMD (*n* = 8) and ART + 3BNC117 + RMD (*n* = 10) on CD3<sup>+</sup> CD8<sup>+</sup> T cells expressing p24. *P* values comparing within groups and between groups were calculated using the paired two-tailed Wilcoxon test and two-tailed Mann–Whitney test, respectively.

**Effect of RMD on active HIV-1-infected cells**

Before analyzing the ‘per RMD’ administration effects on HIV-1 transcriptional activity, we examined the impacts of RMD on CD3<sup>+</sup> CD8<sup>+</sup> p24<sup>+</sup> cells specifically. Overall, we found a significant decrease in CD3<sup>+</sup> CD8<sup>+</sup> p24<sup>+</sup> cells in the ART + RMD group (median reduction, 32%; IQR, 8–70%; *P* = 0.031) during the first 17 days of ART that persisted until day 30 (Fig. 3a; *P* = 0.012). Next, we analyzed changes in the frequency of

CD3<sup>+</sup> CD8<sup>+</sup> T cells expressing mRNA, p24 or both during RMD administration on days 10, 17 and 24 (Fig. 3f and Extended Data Fig. 6). When comparing each pre- to post-RMD infusion time point (1-week interval each), we observed significant median fold increases of 1.78 (IQR, 0.61–3.09; *P* = 0.031) in CD3<sup>+</sup> CD8<sup>+</sup> p24<sup>+</sup> cells (Fig. 3g) and of 1.82 (IQR, 1.14–2.09; *P* = 0.031) in CD3<sup>+</sup> CD8<sup>+</sup> mRNA<sup>+</sup> p24<sup>+</sup> cells after the first infusion and of 1.40 (IQR, 1.08–1.93; *P* = 0.027) in CD3<sup>+</sup> CD8<sup>+</sup> mRNA<sup>+</sup> cells

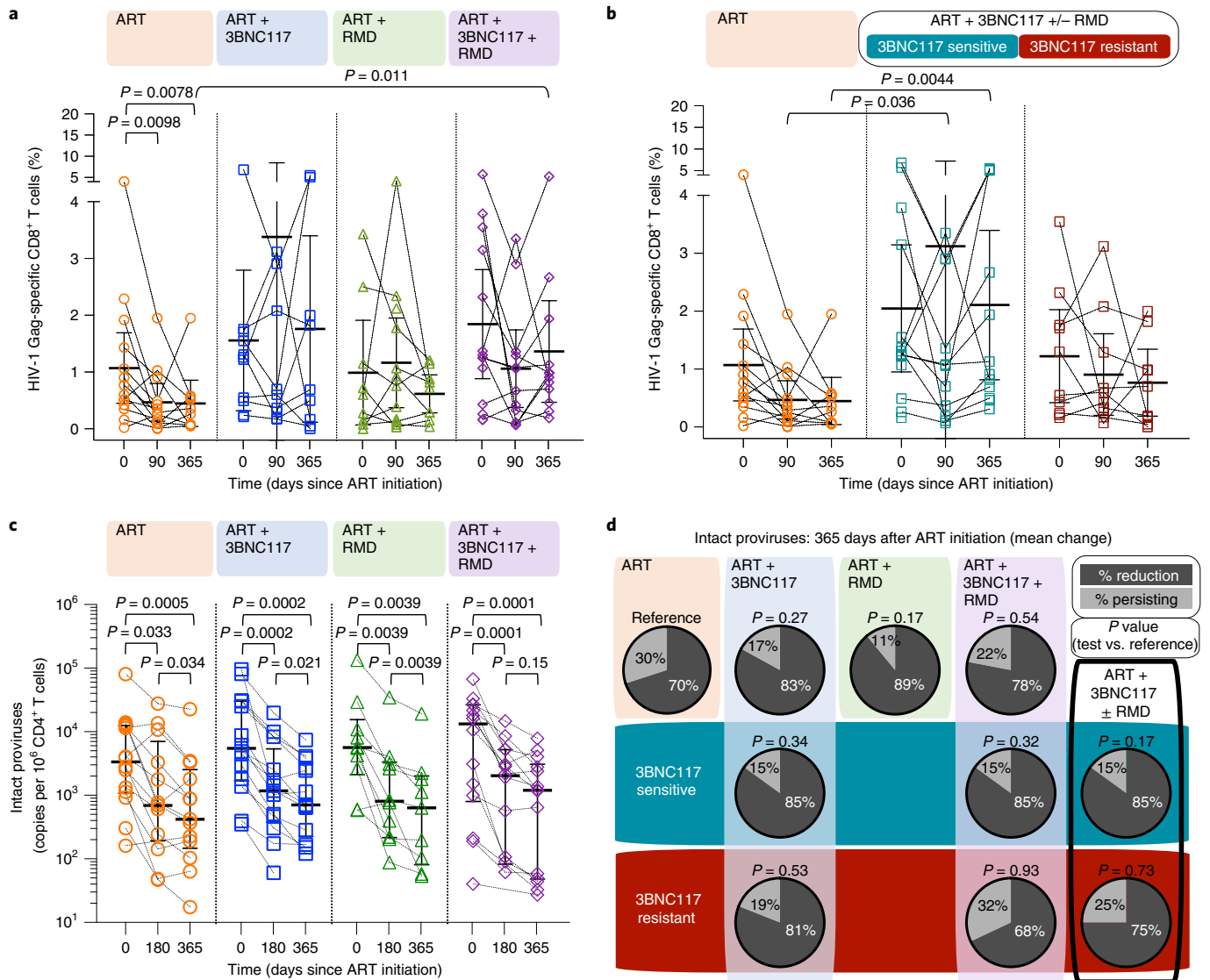


**Fig. 4 | HIV-1 Gag-specific CD8<sup>+</sup> T cell immunity and size of the intact HIV-1 reservoir.** **a**, Dot plot of the frequency of HIV-1 Gag-specific CD8<sup>+</sup> T cells at ART initiation (day 0) and after 90 and 365 days of ART among the four groups (lines at median and IQRs). **b**, Dot plot of the frequency of HIV-1 Gag-specific CD8<sup>+</sup> T cells in groups ART + 3BNC117 ± RMD categorized according to 3BNC117 sensitivity (lines at median and IQRs). **c**, The size of the intact HIV-1 reservoir at ART initiation (day 0) and after 180 and 365 days of ART among individuals in the four randomization groups (lines at median and IQRs). *P* values comparing within groups and between groups were calculated using the paired two-tailed

Wilcoxon test and two-tailed Mann–Whitney test, respectively. **d**, Pie charts showing the mean percentage reduction of intact proviral DNA per 10<sup>6</sup> CD4<sup>+</sup> T cells after 365 days of ART per group (column and upper row) and categorized according to pre-ART plasma virus sensitivity (middle row; blue shaded area) or resistance (bottom row; red shaded area) to 3BNC117. *P* values comparing between groups were calculated using the unpaired two-tailed *t*-test with the ART-only group as reference. The compiled group ART + 3BNC117 ± RMD is shown in the last column. ART, *n* = 14; ART + 3BNC117, *n* = 14; ART + RMD, *n* = 10; ART + 3BNC117 + RMD, *n* = 14.

after the third infusion (Extended Data Fig. 6). Collectively, the data show that RMD administration as latency-reversing therapy during ART initiation modestly yet significantly boosted the number of transcriptionally and/or translationally active HIV-1-infected cells within 1 week of dosing, and this was associated with faster clearance of infected cells at later time points.

**HIV-1 Gag-specific CD8<sup>+</sup> T cell immunity**

We used the activation-induced marker (AIM) assay to investigate HIV-1-specific T cell responses. We noted that the median frequency of HIV-1 Gag-specific CD8<sup>+</sup> T cells over 365 days of ART significantly declined in the ART-only group, as expected following the viral suppression/contraction phase of immunity. In contrast, the median frequency of HIV-1 Gag-specific CD8<sup>+</sup> T cells remained stable over time in the three interventional groups. After 365 days of ART, the median frequency of

HIV-1 Gag-specific CD8<sup>+</sup> T cells in the ART + 3BNC117 + RMD group was higher than that in the ART-only group (0.95% versus 0.31%, respectively; *P* = 0.011) (Fig. 4a). When compared to the ART-only group, the median frequency of HIV-1 Gag-specific CD8<sup>+</sup> T cells on days 90 and 365 was significantly higher in the group that received 3BNC117 with or without RMD and whose pre-ART viruses were sensitive to 3BNC117 (Fig. 4b). Thus, 3BNC117 administration at ART initiation induces durable and potent HIV-1 Gag-specific CD8<sup>+</sup> T cell immune responses.

**Size of the HIV-1 reservoir**

The droplet digital PCR (ddPCR)-based intact proviral DNA assay (IPDA), which simultaneously targets the packaging signal (Ψ) and Rev-responsive element (RRE) regions to identify genomically intact proviruses, can be used to estimate reservoir size in people with HIV-1 subtype B. Because our study population featured both HIV-1 B and

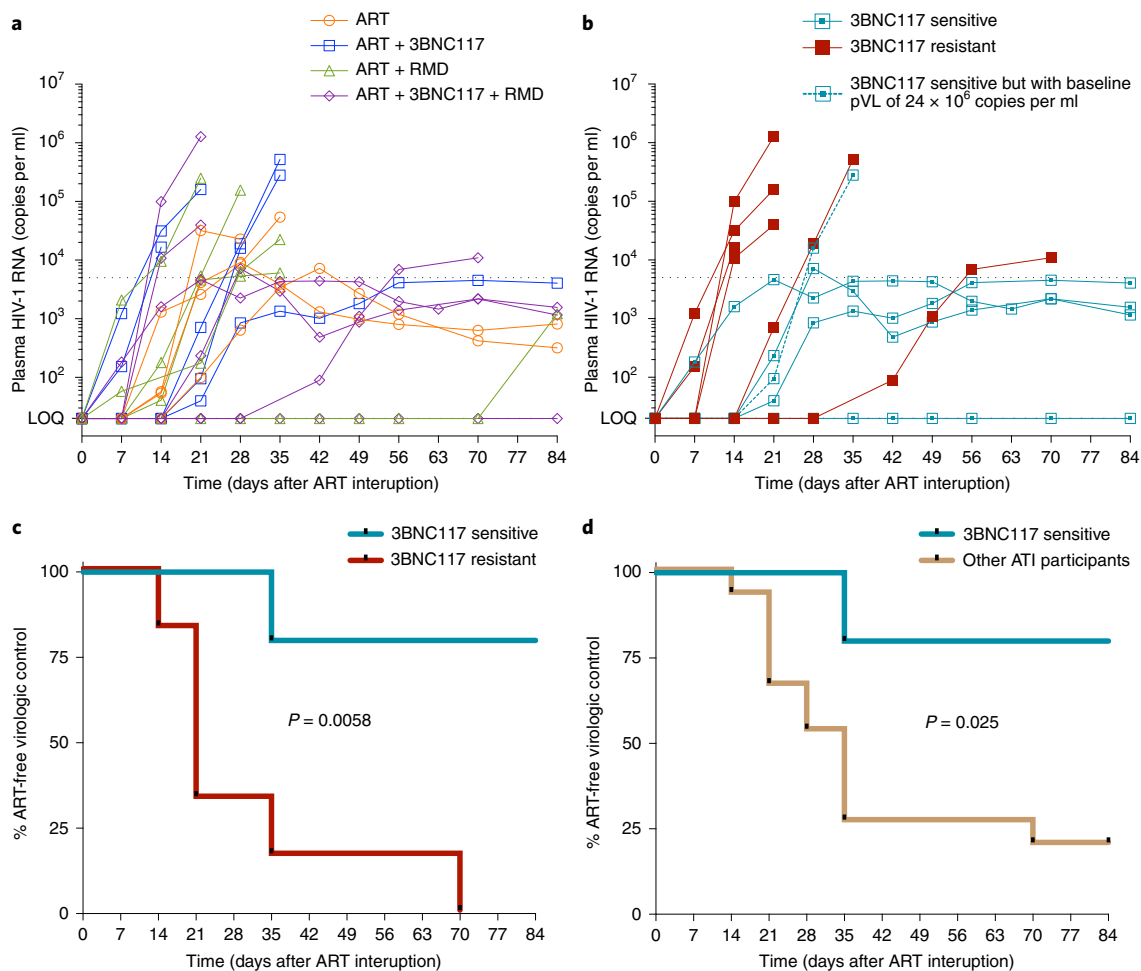


**Fig. 5 | Time to loss of virologic control during 12 weeks of ATI.** **a**, Individual ( $n = 20$ ) plasma HIV-1 RNA levels are shown and coded by group. One individual (ID 125) resumed ART before fulfilling the restarting criteria due to national restrictions during the COVID-19 pandemic. **b**, Individual ( $n = 11$ ) plasma HIV-1 RNA levels for the ART + 3BNC117 and ART + 3BNC117 + RMD groups based on 3BNC117 sensitivity. The horizontal dotted lines indicates plasma HIV-1 RNA at 5,000 copies per ml. **c, d**, Kaplan–Meier curves showing the percentage of

individuals still interrupting ART from day 0 to day 84 during the ATI. Time to loss of virologic control for the ART + 3BNC117 and ART + 3BNC117 + RMD groups based on the 3BNC117-sensitive ( $n = 5$ ) compared to the 3BNC117-resistant ( $n = 6$ ) participants (**c**) and the 3BNC117-sensitive individuals ( $n = 5$ ) compared to the other ATI participants ( $n = 15$ ) (**d**) is shown.  $P$  values were calculated using the log-rank test. pVL, plasma viral load.

non-B subtypes, we performed an IPDA-like duplexed ddPCR (3dPCR) assay that targeted the same  $\Psi$  region as the published IPDA<sup>40</sup> and a region with the RRE, slightly downstream of the original IPDA target region, that has previously been used as a secondary location for this assay<sup>41</sup>. Where necessary, we adapted primer and/or probe sequences to accommodate HIV-1 polymorphisms (Supplementary Table 2). For 23 individuals who harbored the HIV-1 B subtype and for whom a sufficient sample was available, we additionally quantified intact proviruses using the published IPDA<sup>40</sup>. In line with a previous report<sup>41</sup>, IPDA detection failure occurred in 6 (26%) of these 23 individuals, where polymorphism(s) were observed in the IPDA probe(s) and/or at critical primer residue(s) in all cases (Supplementary Table 3). In the remaining 17 individuals, however, the frequency of intact proviruses measured by IPDA correlated strongly with that measured by 3dPCR ( $r = 0.89$ ,  $P < 0.0001$ ; Supplementary Fig. 2), supporting 3dPCR as an accurate method to quantify intact proviral HIV-1 DNA. Using 3dPCR, we observed that the number of proviruses that were positive for both HIV regions and, thus, presumed to be intact varied widely among individuals at baseline (range: 41–134,766 copies per  $10^6$  CD4<sup>+</sup> T cells; Extended Data Table 1), but did not differ between groups ( $P = 0.68$ ) or between HIV-1 B versus non-B subtypes ( $P = 0.60$ ; Supplementary Fig. 3). At baseline, the level of intact proviruses correlated with the

frequency of induced p24<sup>+</sup> CD4<sup>+</sup> T cells, plasma HIV-1 RNA level and CD4<sup>+</sup> T cell count (Supplementary Fig. 1c–e). All four treatment groups had a significant decrease in median intact and defective proviruses from baseline to day 365 (Fig. 4c and Extended Data Fig. 7). The largest median decreases in intact proviruses were observed among the three interventional groups, but there were no significant differences between the groups (Supplementary Table 4). Notably, the observed mean percentage reduction in the frequency of CD4<sup>+</sup> T cells carrying intact provirus was greater for those whose pre-ART plasma viruses were sensitive to 3BNC117 compared to those who harbored resistant viruses (Fig. 4d).

### ART interruption

To determine whether the interventions had an impact on the time to viral rebound, study participants were invited to participate in a closely monitored treatment interruption. Twenty individuals chose to participate in this optional 12-week ATI (Fig. 5a and Extended Data Fig. 1). The baseline characteristics of the ATI participants were comparable to those of the 35 non-ATI participants (Supplementary Table 5). The ATI started day 400 after ART initiation, which was over 1 year after the final 3BNC117 or RMD infusion. Seven of the 20 individuals did not meet the criteria for viral rebound (defined as two consecutive measurements of



>5,000 copies per ml) and displayed partial ART-free virologic control with viremia ranging from <20 to 4,060 copies per ml at week 12 (Fig. 5a and Supplementary Table 6). Of these, one individual (ID 107) in the ART + 3BNC117 + RMD group had complete ART-free virologic control with undetectable plasma HIV-1 RNA throughout the 12 weeks (Fig. 5a and Supplementary Table 6). Among the seven individuals who had negative plasma tests for ART drugs on day 84 of the ATI, two partial controllers had known protective HLA class I alleles: one individual in the ART-only group (ID 707: HLA\*B57, subtype CRF01 and pre-ART plasma HIV-1 RNA of 820 copies per ml) (Extended Data Table 1) and one individual in the ART + 3BNC117 + RMD group (ID 103: HLA\*B27, subtype B and pre-ART plasma HIV-RNA of 730 copies per ml) (Extended Data Table 1). Moreover, of these seven individuals, five were enrolled less than 6 months from their presumed date of HIV-1 infection, which was corroborated by antibody-based recency testing. To investigate whether the sensitivity of pre-ART plasma viruses to 3BNC117 affected time to loss of virologic control during ATI, we divided 3BNC117 recipients who underwent ATI ( $n = 11$ ) into two groups based on 3BNC117 sensitivity (Fig. 5b). Before ATI, individuals harboring pre-ART 3BNC117-sensitive viruses versus those harboring 3BNC117-resistant viruses had a non-significantly higher frequency of HIV-1 Gag-specific CD8<sup>+</sup> T cells and a trend toward lower levels of intact HIV-1 proviruses (Supplementary Table 1). Four of five (80%) individuals with 3BNC117-sensitive pre-ART plasma viruses had ART-free virologic control for 12 weeks, whereas 0 of 6 (0%) individuals with pre-ART 3BNC117-resistant plasma viruses experienced ART-free virologic control (median time to resuming ART, 21 days; IQR, 21–35;  $P = 0.0058$ ) (Fig. 5c). The one 3BNC117-sensitive individual who lost virologic control early on day 35 of the ATI (Fig. 5b) was HIV-1 seronegative at enrollment and had a pre-ART plasma HIV-1 RNA level of 24,000,000 copies per ml (Extended Data Table 1). Because some of the ATI participants not receiving 3BNC117 also had partial ART-free virologic control, we compared 3BNC117-sensitive individuals to all other ATI participants, but the difference in virologic control between the groups remained significant ( $P = 0.025$ ) (Fig. 5d). Of note, no resistance variants against 3BNC117 were identified in rebound viruses from baseline 3BNC117-sensitive individuals during the ATI (Supplementary Fig. 5). Collectively, these findings demonstrate that adjunctive treatment with 3BNC117 at ART initiation led to a high rate of partial or complete ART-free virologic control during treatment interruption among 3BNC117-sensitive individuals more than a year after receiving the antibody.

### Safety

Administration of 3BNC117 and/or RMD was safe and relatively well-tolerated. A total of 319 adverse events (AEs) were registered, of which 205 AEs were determined to be unrelated to the study drugs (Extended Data Table 2). A total of 29 AEs, 27 grade 1 and 2 grade 2, were considered related to 3BNC117, with the most common AEs being fatigue ( $n = 10$ ) and headache ( $n = 7$ ). A total of 85 AEs of which 13 were grade 2 were considered related to RMD with nausea ( $n = 32$ ) and fatigue ( $n = 21$ ) being the most commonly reported. Six serious AEs were observed with none related to either 3BNC117 or RMD (alanine transaminase increase (grade 3), bloodstream infection (grade 3), mental and behavioral disorder due to drug use (grade 2), pregnancy (grade 1), and relapse of psychiatric illness (grade 5); Extended Data Table 2). The median CD4<sup>+</sup> T cell count as well as the CD4/CD8 ratio increased from baseline to day 365 in all four groups during follow-up (Extended Data Fig. 8). Notably, the 13 participants who re-initiated ART during the ATI rapidly achieved viral resuppression (median, 41 days; IQR, 28–56).

### Discussion

In this phase 1b/2a, open-label, multicenter, randomized controlled trial among newly diagnosed individuals initiating ART, we found that early 3BNC117 with or without RMD both enhanced the decay of plasma HIV-1

RNA and facilitated the elimination of HIV-1-infected cells after ART initiation compared with ART alone. We further demonstrated that the observed effects could be directly attributed to the ability of 3BNC117's fragment antigen-binding region to bind to participants' unique viruses, as individuals harboring 3BNC117-sensitive viruses before ART, as predicted by pheno- or genotypic assays, demonstrated significant changes in viral dynamics, HIV-1-specific immune responses and a higher frequency of virologic control following ART interruption. In the optional treatment interruption, four of five (80%) 3BNC117 recipients with pre-ART sensitive plasma viruses maintained ART-free virologic control throughout the 12 weeks of treatment interruption, compared to only 3 of 15 (20%) of those who either had pre-ART 3BNC117-resistant plasma viruses or did not receive 3BNC117. We propose that the superior ART-free virologic control during the ATI among 3BNC117-sensitive individuals could be due to a combination of early targeting of the proviral reservoir and enhanced cellular immune responses.

To our knowledge, no other HIV-1 curative interventions tested in a randomized trial have demonstrated faster decay in plasma viremia, decrease in the frequency of transcriptionally and/or translationally active HIV-1-infected cells and improved virus-specific cellular immunity associated with ART-free virologic control during ART interruption. Therefore, the findings presented in this study are encouraging for the field of HIV-1 cure research.

Of note, 3BNC117 has previously been administered to viremic individuals. A phase 1 trial showed that a single 3BNC117 (30 mg kg<sup>-1</sup>) infusion reduced viremia by a mean of 1.5 log<sub>10</sub> copies per ml among individuals who were not on ART<sup>42</sup>. In this study, as well as in other studies where bNAbs have been administered to ART-naive individuals, bNAb sensitivity was essential for the antiviral efficacy<sup>42–45</sup>. Multiple studies have demonstrated that, in most individuals, circulating viruses develop resistance variants within 1–3 weeks when bNAbs are administered at plasma viral loads above 10<sup>4</sup>–10<sup>5</sup> copies per ml and participants were not on ART<sup>42–45</sup>. In our study, the selection of resistance variants against 3BNC117 was prevented by the co-administration of ART.

Interestingly, early 3BNC117 treatment with or without RMD enhanced the elimination of HIV-1-infected cells during the first phase as well as decay of plasma HIV-1 RNA in the second phase following ART initiation among 3BNC117-sensitive individuals. Integrase-inhibitor-based triple-ART regimens are extremely effective at suppressing plasma viremia in ART-naive individuals, and multiple clinical trials investigating four- or five-drug ART intensification regimens have failed to enhance the suppression of initial viremia compared to integrase-inhibitor-based triple ART alone<sup>46,47</sup>. Thus, it appears that 3BNC117 may mediate its antiviral effects through different mechanisms than regular small molecule antiretroviral drugs. Multiple in vitro and in vivo studies have documented bNAbs' ability to directly neutralize cell-free virus across several HIV-1 subtypes<sup>48,49</sup>. In addition, in vitro and animal experiments indicate that 3BNC117 can enhance the clearance of HIV-1-infected cells through Fc-mediated effector functions<sup>26,50–52</sup>. While it could be argued that the latter effect might primarily target short-lived productively infected cells and not long-term HIV-1 persistence<sup>27,53</sup>, we were able to demonstrate that 3BNC117 mainly eliminated infected cells in the central memory subset—a subset shown to be the main T cell compartment harboring the latent replication-competent HIV-1 reservoir during long-term ART<sup>54–57</sup>. Thus, we conclude that potent bNAbs like 3BNC117 can enhance the elimination of cell-free virus and infected cells among individuals initiating ART through biological mechanisms that differ from those of standard antiretroviral drugs.

Antigen-antibody complexes can form when bNAbs bind to cell-free HIV-1 virus or antigen on the surface of infected cells<sup>27</sup>. These immune complexes stimulate antigen uptake and presentation by antigen-presenting cells in lymphoid tissues, leading to T cell cross-presentation and augmented adaptive HIV-1-specific CD8<sup>+</sup> T cell responses<sup>25</sup>. This antibody-mediated vaccinal effect likely requires

substantial immune complex formation and, thus, an abundance of antigen, which may be why enhancement of HIV-1-specific immunity has not been observed among long-term-suppressed individuals who receive bNAbs in addition to ART<sup>10</sup>. In our study, HIV-1-specific CD8<sup>+</sup> T cell responses were enhanced among 3BNC117-sensitive individuals receiving early 3BNC117 with or without RMD. This maintenance of HIV-1-specific CD8<sup>+</sup> T cell responses after ART initiation might be particularly important to achieve some degree of posttreatment control, as strong CD8<sup>+</sup> T cell immunity has been linked to HIV-1 remission in nonhuman primates and elite controllers<sup>29,31,58</sup>. Furthermore, another recent study demonstrated that maintenance of HIV-1-specific CD8<sup>+</sup> cell responses was directly correlated to the sensitivity of pre-ART plasma viruses to 3BNC117 neutralization<sup>59</sup>. This may explain why circulating autologous nonneutralizing or low-affinity antibodies do not have the same pleiotropic effect on CD8<sup>+</sup> T cells as observed following administration of high-titer potent bNAbs. Of note, increased HIV-1-specific CD8<sup>+</sup> T cell responses have also been observed after the administration of two bNAbs 2 days before and into an ART interruption<sup>29,60</sup>. Thus, our findings suggest that adding bNAbs at ART initiation when plasma viral loads are high might be an effective means of directing and enhancing an individual's CD8<sup>+</sup> T cell immune responses against autologous viruses through immune complex formation and other Fc-mediated effector functions. Whether the higher HIV-1-specific CD8<sup>+</sup> T cell responses observed 1 year after starting ART among bNAb-sensitive individuals receiving early 3BNC117 were caused by higher peak responses, protracted CD8<sup>+</sup> T cell memory contraction or other factors may be explored in future trials.

In this report, we focused primarily on the effect of 3BNC117 with or without RMD administration at ART initiation, but the effectiveness of RMD and other pan-HDACi as LRAs has varied considerably between studies. To our knowledge, our study is the first in which an HDACi has been administered during ART initiation. Consistent with a number of prior studies in long-term ART-treated individuals, we observed modest increases in HIV-1 mRNA and/or p24 expression, from before to after infusion, suggesting RMD-induced HIV-1 expression in infected cells<sup>9–11,21,23</sup>. Additionally, early RMD at ART initiation also led to a faster median daily decay of plasma HIV-1 RNA during the second phase and enhanced clearance of translationally active HIV-1-infected cells during the first 30 days of ART, indicating that early latency reversal can affect the viral reservoir<sup>20,34–37</sup>. However, the ART + RMD group did not experience a delay in time to viral rebound during the ATI, and therefore, the clinical benefits of LRAs at ART initiation, without adding an immunological agent that enhances killing of infected cells, remain uncertain<sup>61</sup>.

Our study also has some limitations and may not be generalizable to all newly diagnosed individuals due to the study's stringent exclusion criteria. For instance, during screening, we excluded 25% of the newly diagnosed individuals due to CD4<sup>+</sup> T cell counts of <200 cells per mm<sup>3</sup>. Less than 50% of the randomized participants underwent ATI, but, notably, the characteristics of those who interrupted ART were not different from those who did not interrupt ART, suggesting that outcomes observed among ATI participants were likely generalizable to the total study population. Additionally, our analyses were done on peripheral blood, but it would be of great interest to compare these findings to complementary analyses performed on tissue samples, for example, lymphatic tissues<sup>62</sup>, in future studies. Finally, the findings from this clinical study need to be verified on a larger scale to increase both generalizability and statistical power.

In conclusion, our findings suggest that administration of 3BNC117 at the time of ART initiation reduced the number of transcriptionally active HIV-1-infected cells, resulted in a faster decay of plasma HIV-1 RNA and increased HIV-1 CD8<sup>+</sup> T cell immunity, compared to ART alone. Our findings are consistent with the observation that bNAb administration during ART interruption may accelerate reservoir decay<sup>63</sup>. Notably, co-administration of 3BNC117 with or without RMD at ART initiation led to prolonged ART-free virologic control during treatment interruption

in a subset of individuals whose pre-ART viruses were sensitive to the bNAb. Collectively, the findings strongly support the further development of interventions administered at the time of ART initiation as a strategy to limit long-term HIV-1 persistence.

## Online content

Any methods, additional references, Nature Research reporting summaries, source data, extended data, supplementary information, acknowledgements, peer review information; details of author contributions and competing interests; and statements of data and code availability are available at <https://doi.org/10.1038/s41591-022-02023-7>.

## References

1. Abrahams, M. R. et al. The replication-competent HIV-1 latent reservoir is primarily established near the time of therapy initiation. *Sci. Transl. Med.* **11**, eaaw5589 (2019).
2. Brodin, J. et al. Establishment and stability of the latent HIV-1 DNA reservoir. *elife* **5**, e18889 (2016).
3. Martin, G. E. et al. Levels of human immunodeficiency virus DNA are determined before ART initiation and linked to CD8 T-cell activation and memory expansion. *J. Infect. Dis.* **221**, 1135–1145 (2020).
4. Jones, B. R. et al. Phylogenetic approach to recover integration dates of latent HIV sequences within-host. *Proc. Natl Acad. Sci. USA* **115**, E8958–E8967 (2018).
5. Brooks, K. et al. HIV-1 variants are archived throughout infection and persist in the reservoir. *PLoS Pathog.* **16**, e1008378 (2020).
6. Rasmussen, T. A. et al. Panobinostat, a histone deacetylase inhibitor, for latent-virus reactivation in HIV-infected patients on suppressive antiretroviral therapy: a phase 1/2, single group, clinical trial. *Lancet HIV* **1**, e13–e21 (2014).
7. Li, J. Z. et al. The size of the expressed HIV reservoir predicts timing of viral rebound after treatment interruption. *AIDS* **30**, 343–353 (2016).
8. Kroon, E. D. M. B. et al. A randomized trial of vorinostat with treatment interruption after initiating antiretroviral therapy during acute HIV-1 infection. *J. Virus Erad.* **6**, 100004 (2020).
9. Leth, S. et al. Combined effect of Vacc-4x, recombinant human granulocyte macrophage colony-stimulating factor vaccination, and romidepsin on the HIV-1 reservoir (REDUC): a single-arm, phase 1B/2A trial. *Lancet HIV* **3**, e463–e472 (2016).
10. Gruell, H. et al. Effect of 3BNC117 and romidepsin on the HIV-1 reservoir in people taking suppressive antiretroviral therapy (ROADMAP): a randomised, open-label, phase 2A trial. *Lancet Microbe* **3**, e203–e214 (2022).
11. Søgaard, O. S. et al. The depsipeptide romidepsin reverses HIV-1 latency in vivo. *PLoS Pathog.* **11**, e1005142 (2015).
12. Lehrman, G. et al. Depletion of latent HIV-1 infection in vivo: a proof-of-concept study. *Lancet* **366**, 549–555 (2005).
13. Archin, N. M. et al. Valproic acid without intensified antiviral therapy has limited impact on persistent HIV infection of resting CD4<sup>+</sup> T cells. *AIDS* **22**, 1131–1135 (2008).
14. Archin, N. M. et al. Antiretroviral intensification and valproic acid lack sustained effect on residual HIV-1 viremia or resting CD4<sup>+</sup> cell infection. *PLoS ONE* **5**, e9390 (2010).
15. Routy, J. P. et al. Design and implementation of a randomized crossover study of valproic acid and antiretroviral therapy to reduce the HIV reservoir. *HIV Clin. Trials* **13**, 301–307 (2012).
16. Archin, N. M. et al. Administration of vorinostat disrupts HIV-1 latency in patients on antiretroviral therapy. *Nature* **487**, 482–485 (2012).
17. Elliott, J. H. et al. Activation of HIV transcription with short-course vorinostat in HIV-infected patients on suppressive antiretroviral therapy. *PLoS Pathog.* **10**, e1004473 (2014).

18. Archin, N. M. et al. HIV-1 expression within resting CD4<sup>+</sup> T cells after multiple doses of vorinostat. *J. Infect. Dis.* **210**, 728–735 (2014).
19. Wei, D. G. et al. Histone deacetylase inhibitor romidepsin induces HIV expression in CD4 T cells from patients on suppressive antiretroviral therapy at concentrations achieved by clinical dosing. *PLoS Pathog.* **10**, e1004071 (2014).
20. Gunst, J. D., Tolstrup, M., Rasmussen, T. A. & Søgaard, O. S. The potential role for romidepsin as a component in early HIV-1 curative efforts. *Expert Rev. Anti. Infect. Ther.* **14**, 447–450 (2016).
21. McMahon, D. K. et al. A phase 1/2 randomized, placebo-controlled trial of romidespin in persons with HIV-1 on suppressive antiretroviral therapy. *J. Infect. Dis.* **224**, 648–656 (2021).
22. Shan, L. et al. Stimulation of HIV-1-specific cytolytic T lymphocytes facilitates elimination of latent viral reservoir after virus reactivation. *Immunity* **36**, 491–501 (2012).
23. Mothe, B. et al. HIVconsv vaccines and romidepsin in early-treated HIV-1-infected individuals: safety, immunogenicity and effect on the viral reservoir (Study BCN02). *Front. Immunol.* **11**, 823 (2020).
24. Fidler, S. et al. Antiretroviral therapy alone versus antiretroviral therapy with a kick and kill approach, on measures of the HIV reservoir in participants with recent HIV infection (the RIVER trial): a phase 2, randomised trial. *Lancet* **395**, 888–898 (2020).
25. Caskey, M., Klein, F. & Nussenzweig, M. C. Broadly neutralizing anti-HIV-1 monoclonal antibodies in the clinic. *Nat. Med.* **25**, 547–553 (2019).
26. Lu, C.-L. et al. Enhanced clearance of HIV-1-infected cells by broadly neutralizing antibodies against HIV-1 in vivo. *Science* **352**, 1001–1004 (2016).
27. Dufloo, J. et al. Broadly neutralizing anti-HIV-1 antibodies tether viral particles at the surface of infected cells. *Nat. Commun.* **13**, 630 (2022).
28. Schoofs, T. et al. HIV-1 therapy with monoclonal antibody 3BNC117 elicits host immune responses against HIV-1. *Science* **352**, 997–1001 (2016).
29. Niessl, J. et al. Combination anti-HIV-1 antibody therapy is associated with increased virus-specific T cell immunity. *Nat. Med.* **26**, 222–227 (2020).
30. Scheid, J. F. et al. Sequence and structural convergence of broad and potent HIV antibodies that mimic CD4 binding. *Science* **333**, 1633–1637 (2011).
31. Nishimura, Y. et al. Early antibody therapy can induce long-lasting immunity to SHIV. *Nature* **543**, 559–563 (2017).
32. DiLillo, D. J. & Ravetch, J. V. Differential Fc-receptor engagement drives an anti-tumor vaccinal effect. *Cell* **161**, 1035–1045 (2015).
33. Gay, C. L. et al. Stable latent HIV infection and low-level viremia despite treatment with the broadly neutralizing antibody VRC07-523LS and the latency reversal agent vorinostat. *J. Infect. Dis.* **225**, 856–861 (2022).
34. Gunst, J. D., Tolstrup, M. & Søgaard, O. S. Beyond antiretroviral therapy: early interventions to control HIV-1 infection. *AIDS* **31**, 1665–1667 (2017).
35. Reece, J. et al. An ‘escape clock’ for estimating the turnover of SIV DNA in resting CD4<sup>+</sup> T cells. *PLoS Pathog.* **8**, e1002615 (2012).
36. Reece, J. C. et al. Measuring turnover of SIV DNA in resting CD4<sup>+</sup> T cells using pyrosequencing: implications for the timing of HIV eradication therapies. *PLoS ONE* **9**, e93330 (2014).
37. Petracic, J., Martyushev, A., Reece, J. C., Kent, S. J. & Davenport, M. P. Modeling the timing of antilateness drug administration during HIV treatment. *J. Virol.* **88**, 14050–14056 (2014).
38. Baxter, A. E. et al. Multiparametric characterization of rare HIV-infected cells using an RNA-flow FISH technique. *Nat. Protoc.* **12**, 2029–2049 (2017).
39. Puertas, M. C. et al. VIP-SPOT: an innovative assay to quantify the productive HIV-1 reservoir in the monitoring of cure strategies. *mBio* **12**, e0056021 (2021).
40. Bruner, K. M. et al. A quantitative approach for measuring the reservoir of latent HIV-1 proviruses. *Nature* **566**, 120–125 (2019).
41. Kinloch, N. N. et al. HIV-1 diversity considerations in the application of the Intact Proviral DNA Assay (IPDA). *Nat. Commun.* **12**, 165 (2021).
42. Caskey, M. et al. Viraemia suppressed in HIV-1-infected humans by broadly neutralizing antibody 3BNC117. *Nature* **522**, 487–491 (2015).
43. Bar-On, Y. et al. Safety and antiviral activity of combination HIV-1 broadly neutralizing antibodies in viremic individuals. *Nat. Med.* **24**, 1701–1707 (2018).
44. Stephenson, K. E. et al. Safety, pharmacokinetics and antiviral activity of PGT121, a broadly neutralizing monoclonal antibody against HIV-1: a randomized, placebo-controlled, phase 1 clinical trial. *Nat. Med.* **27**, 1718–1724 (2021).
45. Caskey, M. et al. Antibody 10-1074 suppresses viremia in HIV-1-infected individuals. *Nat. Med.* **23**, 185–191 (2017).
46. Feng, Q. et al. Quadruple versus triple combination antiretroviral therapies for treatment naive people with HIV: systematic review and meta-analysis of randomised controlled trials. *Br. Med. J.* **366**, 4179 (2019).
47. Markowitz, M. et al. A randomized open-label study of 3- versus 5-drug combination antiretroviral therapy in newly HIV-1-infected individuals. *J. Acquir. Immune Defic. Syndr.* **66**, 140–147 (2014).
48. Scheid, J. F. et al. Sequence and structural convergence. *Science* **333**, 1633–1637 (2011).
49. Stefic, K., Bouvin-Pley, M., Braibant, M. & Barin, F. Impact of HIV-1 diversity on its sensitivity to neutralization. *Vaccines* **7**, 74 (2019).
50. Wang, P. et al. Quantifying the contribution of Fc-mediated effector functions to the antiviral activity of anti-HIV-1 IgG1 antibodies in vivo. *Proc. Natl Acad. Sci. USA* **117**, 18002–18009 (2020).
51. Asokan, M. et al. Fc-mediated effector function contributes to the in vivo antiviral effect of an HIV neutralizing antibody. *Proc. Natl Acad. Sci. USA* **117**, 18754–18763 (2020).
52. Veenhuis, R. T., Garliss, C. C., Bailey, J. R. & Blankson, J. N. CD8 effector T cells function synergistically with broadly neutralizing antibodies to enhance suppression of HIV infection. *Front. Immunol.* **12**, 708355 (2021).
53. Spencer, D. A. et al. Phagocytosis by an HIV antibody is associated with reduced viremia irrespective of enhanced complement lysis. *Nat. Commun.* **13**, 662 (2022).
54. Chomont, N. et al. HIV reservoir size and persistence are driven by T cell survival and homeostatic proliferation. *Nat. Med.* **15**, 893–900 (2009).
55. Hiener, B. et al. Identification of genetically intact HIV-1 proviruses in specific CD4<sup>+</sup> T cells from effectively treated participants. *Cell Rep.* **21**, 813–822 (2017).
56. Buzon, M. J. et al. HIV-1 persistence in CD4<sup>+</sup> T cells with stem cell-like properties. *Nat. Med.* **20**, 139–142 (2014).
57. Jaafoura, S. et al. Progressive contraction of the latent HIV reservoir around a core of less-differentiated CD4<sup>+</sup> memory T cells. *Nat. Commun.* **5**, 5407 (2014).
58. Collins, D. R., Gaiha, G. D. & Walker, B. D. CD8<sup>+</sup> T cells in HIV control, cure and prevention. *Nat. Rev. Immunol.* **20**, 471–482 (2020).
59. Rosás-Umbert, M. et al. Administration of broadly neutralizing anti-HIV-1 antibodies at ART initiation maintains long-term CD8<sup>+</sup> T cell immunity. *Nat. Commun.* (in the press).

60. Mendoza, P. et al. Combination therapy with anti-HIV-1 antibodies maintains viral suppression. *Nature* **561**, 479–484 (2018).
61. Deeks, S. G. et al. Research priorities for an HIV cure: International AIDS Society global scientific strategy 2021. *Nat. Med.* **27**, 2085–2098 (2021).
62. Estes, J. D. et al. Defining total-body AIDS-virus burden with implications for curative strategies. *Nat. Med.* **23**, 1271–1276 (2017).
63. Gaebler, C. et al. Prolonged viral suppression with anti-HIV-1 antibody therapy. *Nature* **606**, 368–374 (2022).

**Publisher's note** Springer Nature remains neutral with regard to jurisdictional claims in published maps and institutional affiliations.

Springer Nature or its licensor holds exclusive rights to this article under a publishing agreement with the author(s) or other rightsholder(s); author self-archiving of the accepted manuscript version of this article is solely governed by the terms of such publishing agreement and applicable law.

© The Author(s), under exclusive licence to Springer Nature America, Inc. 2022

**Jesper D. Gunst**<sup>1,2</sup>, **Marie H. Pahu**<sup>1,2</sup>, **Miriam Rosás-Umbert**<sup>1,2</sup>, **I-Na Lu**<sup>3</sup>, **Thomas Benfield**<sup>4</sup>, **Henrik Nielsen**<sup>5,6</sup>, **Isik S. Johansen**<sup>7</sup>, **Rajesh Mohey**<sup>8</sup>, **Lars Østergaard**<sup>1,2</sup>, **Vibeke Klastrup**<sup>2</sup>, **Maryam Khan**<sup>9,10</sup>, **Mariane H. Schleimann**<sup>1,2</sup>, **Rikke Olesen**<sup>1,2</sup>, **Henrik Støvring**<sup>11</sup>, **Paul W. Denton**<sup>12</sup>, **Natalie N. Kinloch**<sup>13,14</sup>, **Dennis C. Copertino**<sup>15,16</sup>, **Adam R. Ward**<sup>15</sup>, **Winiffer D. Conce Alberto**<sup>15,16</sup>, **Silke D. Nielsen**<sup>1,2</sup>, **Maria C. Puertas**<sup>17,18</sup>, **Victor Ramos**<sup>19</sup>, **Jacqueline D. Reeves**<sup>20</sup>, **Christos J. Petropoulos**<sup>20</sup>, **Javier Martinez-Picado**<sup>17,18,21,22</sup>, **Zabrina L. Brumme**<sup>13,14</sup>, **R. Brad Jones**<sup>15,16</sup>, **Julie Fox**<sup>23,24</sup>, **Martin Tolstrup**<sup>1,2</sup>, **Michel C. Nussenzweig**<sup>19,25</sup>, **Marina Caskey**<sup>19</sup>, **Sarah Fidler**<sup>9,10</sup> and **Ole S. Søgaard**<sup>1,2</sup> ✉

<sup>1</sup>Department of Clinical Medicine, Aarhus University, Aarhus, Denmark. <sup>2</sup>Department of Infectious Diseases, Aarhus University Hospital, Aarhus, Denmark. <sup>3</sup>Department of Neurology with Institute of Translational Neurology, University Hospital Münster, Münster, Germany. <sup>4</sup>Department of Infectious Diseases, Copenhagen University Hospital–Amager and Hvidovre, Hvidovre, Denmark. <sup>5</sup>Department of Infectious Diseases, Aalborg University Hospital, Aalborg, Denmark. <sup>6</sup>Department of Clinical Medicine, Aalborg University, Aalborg, Denmark. <sup>7</sup>Department of Infectious Diseases, Odense University Hospital, University of Southern Denmark, Odense, Denmark. <sup>8</sup>Department of Internal Medicine, Regional Hospital Herning, Herning, Denmark. <sup>9</sup>Department of Infectious Diseases, Imperial College Hospital, London, UK. <sup>10</sup>The National Institute for Health Research, Imperial Biomedical Research Centre, London, UK. <sup>11</sup>Department of Public Health, Aarhus University, Aarhus, Denmark. <sup>12</sup>Department of Biology, University of Nebraska at Omaha, Omaha, NE, USA. <sup>13</sup>Faculty of Health Sciences, Simon Fraser University, Burnaby, British Columbia, Canada. <sup>14</sup>British Columbia Centre for Excellence in HIV/AIDS, Vancouver, British Columbia, Canada. <sup>15</sup>Infectious Diseases Division, Department of Medicine, Weill Cornell Medical College, New York, NY, USA. <sup>16</sup>Department of Microbiology and Immunology, Weill Cornell Graduate School of Medical Sciences, New York, NY, USA. <sup>17</sup>IrsiCaixa AIDS Research Institute, Badalona, Spain. <sup>18</sup>CIBERINFEC, Madrid, Spain. <sup>19</sup>Laboratory of Molecular Immunology, The Rockefeller University, New York, NY, USA. <sup>20</sup>Labcorp-Monogram Biosciences, South San Francisco, CA, USA. <sup>21</sup>University of Vic–Central University of Catalonia, Vic, Spain. <sup>22</sup>Catalan Institution for Research and Advanced Studies, Barcelona, Spain. <sup>23</sup>Department of Genitourinary Medicine and Infectious Disease, Guy's and St Thomas' National Health Service Trust, London, UK. <sup>24</sup>Department of Genitourinary Medicine and Infectious Disease, The National Institute for Health Research Biomedical Research Centre, King's College London, London, UK. <sup>25</sup>Howard Hughes Medical Institute, The Rockefeller University, New York, NY, USA.

✉e-mail: [olesoega@rm.dk](mailto:olesoega@rm.dk)

## Methods

### Study design

This was a phase 1b/2a, open-label, multicenter, randomized controlled trial enrolling at five sites in Denmark and two sites in the United Kingdom. Before any study-related procedures, written informed consent was obtained from the participant. Participants were randomized into one of four groups: ART alone, ART + 3BNC117, ART + RMD or ART + 3BNC117 + RMD in a 1:1:1:1 ratio (Fig. 1a,b). Screening occurred within 4 weeks before the baseline visit at day 0. Participants were followed until day 365 of ART or longer if they chose to enroll in the optional 12-week ATI at day 400. The study was conducted in accordance with Good Clinical Practice and reported in accordance with the CONSORT 2010 statement<sup>64</sup>. The protocol was approved by the Danish Medicine Authorities in Denmark and the Medicines (2016053184) and Healthcare Products (31883/0001/001-0001) Regulatory Agency in the United Kingdom, as well as the National Committee on Health Research Ethics in Denmark (1-10-72-110-16) and National Health Authority in the United Kingdom (241439). Study data were collected and managed in Research Electronic Data Capture (REDCap) electronic data capture tools hosted at the Clinical Trial Unit, Department of Clinical Medicine, Aarhus University, Aarhus, Denmark<sup>65,66</sup>. The study was monitored by the Danish Good Clinical Practice Units (<https://gcp-enhed.dk/english/>) from screening to the final visit.

### Participants

Newly diagnosed ART-naive participants aged 18 or above with a confirmed HIV-1 diagnosis and a CD4<sup>+</sup> T cell count of >200 cells per mm<sup>3</sup> at screening were recruited by study physicians. All participants initially received integrase-inhibitor-based ART regimens. Participants were reimbursed for transport expenses relating to the study but otherwise did not receive any financial compensation for participating in the study except compensation for lost earnings during study visits. Detailed inclusion and exclusion criteria can be found in the protocol: eCLEAR-001, version 3.1, 18 September 2018.

### Randomization

The Clinical Trial Unit at Aarhus University generated the randomization sequence using permuted blocks of four or eight by computer-generated random numbers without stratification to sex and age. Randomization assignment was provided to each site using REDCap.

### Procedures

3BNC117 was administered intravenously at a dose of 30 mg kg<sup>-1</sup> over 60 min at days 7 ± 3 and 21 ± 3 after ART initiation. 3BNC117 dosing was based on the previously observed antiviral efficacy in clinical studies<sup>42,43,60</sup>. RMD (Bristol-Myers Squibb) at 5 mg per m<sup>2</sup> was administered intravenously over 120 min at days 10 ± 3, 17 ± 3 and 24 ± 3 after ART initiation. RMD dosing was based on the previously observed latency reversal in clinical studies<sup>9,11,23</sup>. Study participants were monitored with vital signs before, during and for 1 h after each infusion. Premedication with ondansetron 8 mg orally was offered as prophylactic antiemetic treatment at least 30 min before each RMD infusion. The infusion visits in Denmark were completed at the Clinical Research Unit at Aarhus University Hospital or Hvidovre Hospital and in the United Kingdom were done at the National Institute for Health Research, Imperial Clinical Research Facility or the Clinical Research Facility, Guy's and St. Thomas' Biomedical Research Center. Follow-up visits were completed at the respective outpatient clinics of participating hospitals. Blood samples were collected at days 0, 7, 10, 17, 21, 24 (including postinfusion samples at the end of 2 h of infusion for RMD recipients at days 10, 17 and 24), 30, 60, 90, 180, 270 and 365 after ART initiation. Blood samples were processed within 4 h of collection, and serum and plasma samples were stored at -80 °C. Peripheral blood mononuclear cells (PBMCs) were isolated by density gradient centrifugation and cryopreserved in

FBS with 10% dimethyl sulfoxide (DMSO). Clinical safety assessments included directed physical examinations, vital sign measurement, and review of AEs and concomitant medications at every visit and reported until the end of the study (Fig. 1a). The Common Terminology Criteria for Adverse Events (CTCAE) v4.03 grading scale was used to grade AEs. No safety monitoring committee was involved because the interventional period was relatively short and the study drugs were well-characterized. Safety biochemistry was taken at days -28 to 0, 7, 10, 17, 21, 24 and 365 after ART initiation. Plasma HIV-1 RNA levels were measured with standardized clinical assays at every visit. CD4<sup>+</sup> T cell counts were measured on days -28 to -1, baseline (day 0), 10, 17, 24, 30, 90, 180, 270 and 365. Of the 52 individuals who could participate in the optional ATI, only 20 individuals participated, 29 individuals were not willing to participate due to personal reasons and 3 individuals were willing, but not eligible for participation (Extended Data Fig. 1). During ATI, plasma HIV-1 RNA levels, CD4<sup>+</sup> T cell counts and safety assessments were conducted every week for the first 8 weeks and, subsequently, biweekly. After the resumption of ART, we monitored plasma HIV-1 RNA levels every fourth week until levels were undetectable (<20 copies per ml) on two consecutive measurements. We acknowledge the lack of a data and safety monitoring board, but the study design allowed designated investigators at each site with access to all data. All safety data and medical notes were monitored by external monitors from the Danish Good Clinical Practice Units.

### HIV-1-infected cells using the FISH-flow assay

Multiparametric characterization of the transcriptional and/or translational activity of HIV-1-infected cells was done using a Human Prime-Flow RNA Assay Kit (AH Diagnostics) according to a well-established HIV-1 RNA FISH-flow assay protocol<sup>38</sup>. We used samples from the interventional period in a subset of participants at five or eight time points: baseline (day 0) and days 10, 17, 24, (+ three postinfusion time points for RMD recipients) and 30 after ART initiation. To ensure the collection of  $3 \times 10^6$  cells at the final step of acquisition on the flow cytometer, we began with at least  $3 \times 10^7$  frozen PBMCs from the individuals at each time point. Samples obtained at different time points that derived from the same individual were always assayed simultaneously using identical reagent master mixes to minimize any potential batch effect. Only singlet, live cells were included in the data analyses. Samples were gated on CD3<sup>+</sup> CD8<sup>-</sup> T cells due to downregulation of CD4: lymphocytes > single cells (forward scatter) > single cells (side scatter) > live CD3<sup>+</sup> cells > CD8<sup>-</sup> cells > HIV-1 RNA<sup>+</sup> and Gag p24<sup>+</sup> cells (Supplementary Fig. 4). Transcriptionally active HIV-1-infected cells were identified as HIV-1 mRNA<sup>+</sup>. HIV-1-infected cells both transcriptionally and translationally active were identified as HIV-1 mRNA<sup>+</sup> and Gag p24<sup>+</sup>. Translationally active HIV-1-infected cells were identified as Gag p24<sup>+</sup>. Due to a faulty mRNA probe in the second batch of FISH-flow analyses, mRNA data were only available for half of the study population analyzed by FISH-flow assay (Fig. 1b). Of note, the analyses were not done on specific selected individuals, but on all individuals for whom we had sufficient quantities of cryopreserved PBMCs (with viability >70% after thawing and resting) at multiple study time points during the first 30 days after starting ART. The FISH-flow assay was validated based on the correlations between CD3<sup>+</sup> CD8<sup>-</sup> T cells expressing mRNA, p24 or both and plasma HIV-1 RNA<sup>67,68</sup>, CD4<sup>+</sup> T cell count<sup>67,68</sup> and the CD4/CD8 ratio<sup>68</sup>. Memory subsets within CD3<sup>+</sup> CD8<sup>-</sup> T cells were defined based on CD27 and CD45RA expression: central memory T cells (T<sub>CM</sub>), CD27<sup>+</sup> CD45RA<sup>-</sup>; naive T cells (T<sub>N</sub>), CD27<sup>+</sup> CD45RA<sup>+</sup>; effector memory T cells (T<sub>EM</sub>), CD27<sup>-</sup> CD45RA<sup>+</sup>; and terminally differentiated T cells (T<sub>TD</sub>). T follicular helper (T<sub>FH</sub>) cells were defined based on CXCR5 and PD-1 expression. The immunofluorescent monoclonal antibodies BUV395-CD4 (clone SK3), BUV496-CD8 (clone RPA-T8), BUV737-CD3 (clone UCHT1), BV605-CD27 (clone L128), BV786-Ki-67 (clone B56) and BB515-CD185 (CXCR5) (clone: RF8B2) were purchased from BD Pharmingen. The Human TruStain FcX, BV711-CD45RA (clone HI100),

PE-Cy7-PD-1 (clone EH12.2H7) and Zombie Violet were purchased from BioLegend. For labeling HIV-1 Gag p24 protein, cells were intracellularly stained with PE-P24 (clone KC57-RD1, Beckman Coulter). All the samples were analyzed on an LSRFortessa X-20 Flow Cytometer (BD Biosciences) and flow cytometry data were analyzed using FlowJo software, version 10.6.0 (Tree Star).

### HIV-1-specific CD8<sup>+</sup> T cell immunity using the AIM assay

We assessed HIV-1-specific CD8<sup>+</sup> T cell immunity using the AIM assay by flow cytometry at baseline (day 0) and days 90 and 365 after ART initiation. Cryopreserved PBMCs were thawed, washed and rested at 37 °C for 3 h. Cells were then plated into the wells of a 96-well plate, at a total of  $1 \times 10^6$  cells per well. For each assay, five conditions were used including no exogenous stimulation with DMSO as negative control, four HIV-1 antigen stimulations and staphylococcal enterotoxin B (SEB,  $1 \mu\text{g ml}^{-1}$ ) as positive control. The antigen stimulations were overlapping peptide pools corresponding to HIV Gag (JPT, PM-HIV-Gag), HIV Env (JPT, PM-HIV-ENV), HIV Nef (JPT, PM-HIV-Nef) and HIV Pol (JPT, PM-HIV-Pol) used at a final concentration of  $2 \mu\text{g ml}^{-1}$  of total peptide. Following 20 h of incubation at 37 °C, cells were washed with PBS and stained for viability with Near IR Dead Live Dead for 20 min. Cells were then incubated with Human TruStain FcX (BioLegend) in PBS with 2% FBS for 10 min and stained for 30 min with surface markers-specific antibodies: CD3 (PerCP/Cy5.5 anti-human CD3, SK7, BioLegend), CD4 (BV650 anti-human CD4, RPA-T4, BioLegend), CD8 (BV605 anti-human CD8a, RPA-T8, BioLegend), 4-1BB (PE anti-human CD137, BioLegend), CD69 (APC anti-human CD69, FN50, BioLegend) and PD-L1 (BV421 anti-human CD274, B7-H1, BioLegend). Cells were washed twice and acquired on a MACSQuant16. Data were analyzed using FlowJo 10.6.0. The frequency of antigen-specific cells (AIM<sup>+</sup> cells) was determined by subtracting the frequency in the nonstimulation condition from the antigen-stimulated conditions. AIM<sup>+</sup> cells were considered as the sum of the frequency of cells that were CD69<sup>+</sup>PD-L1<sup>+</sup>4-1BB<sup>+</sup>, CD69<sup>+</sup>PD-L1<sup>+</sup>CD69<sup>+</sup>4-1BB<sup>+</sup> or PD-L1<sup>+</sup>4-1BB<sup>+</sup>. Total HIV-1-specific AIM<sup>+</sup> cells were calculated as the sum of each of the four populations for the four antigen stimulations. In this paper, we report the HIV-1 Gag-specific CD8<sup>+</sup> T cell immunity only, whereas a detailed description of the HIV-1-specific T cell immunity will be reported separately<sup>59</sup>.

### Intact HIV-1 proviruses by 3dPCR

We applied a 3dPCR assay adapted from the IPDA protocol, which is specific for HIV-1 subtype B<sup>40</sup>. Duplexing increases the selectivity of molecular assays to identify genomically intact proviruses, particularly when primer–probe sets are placed in locations that are highly predictive of proviral integrity. The IPDA achieves this by targeting  $\Psi$  and RRE, which are frequently deleted or mutated in defective proviruses<sup>40</sup>. As a substantial proportion of individuals harbored non-B infections, we performed an IPDA-like 3dPCR assay that leverages these principles, using autologous primers and probes, which were necessary to accommodate HIV polymorphism. The two HIV regions targeted by the 3dPCR assay were the  $\Psi$  region featured in the published IPDA<sup>40</sup> and a region within the RRE in *env*, located slightly downstream of the original IPDA *env* primer–probe set, that has previously been used as a secondary ('backup') location for this assay<sup>41</sup>. The published primer and probe sequences for these regions are as follows: HIV-1  $\Psi$  forward primer, 5'-CAGGACTCGGCTTGCTGAAG-3'; HIV-1  $\Psi$  probe, 5'-FAM-TTTTGGCGTACTCACCAGT-MGBNFQ-3'; HIV-1  $\Psi$  reverse primer, 5'-GCACCATCTCTCTCTTCTAGC-3'; HIV-1 secondary *env* forward primer, 5'-ACTATGGGCGCAGCGTC-3'; HIV-1 secondary *env* probe, 5'-VIC-CTGGCCTGACCGTACG-MGBNFQ-3'; and HIV-1 secondary *env* reverse primer, 5'-CCCCAGACTGTGAGTTGCA-3' (Supplementary Table 2). While the 3dPCR assay has not been formally validated to the same extent as the IPDA for genomic integrity prediction, the two assays feature identical 5' primer–probe locations in  $\Psi$ , and partially overlapping 3' primer–probe locations in *env*, where the latter are

situated within a region that is highly predictive of intact proviruses, at least in HIV-1 subtype B<sup>40</sup>.

To assess whether the published primers and probes were appropriate for each participant or whether autologous oligonucleotide design would be required, we sequenced the  $\Psi$  and *env* assay regions from pre-ART plasma HIV-1 RNA samples for all participants for whom samples were available for 3dPCR. Plasma HIV-1 RNA was sequenced so that any autologous primers and probes would capture intact HIV sequences to guide oligonucleotide design. Briefly, single-template amplification and sequencing were performed for *env* with gene-specific primers as described below. For  $\Psi$ , RNA extraction and cDNA synthesis were performed as for *env* with the gene-specific primer 2crx: 5'-TAACCCTGCGGGATGTGGTATTCC-3'. Bulk nested PCR was conducted with Platinum Taq DNA polymerase High Fidelity (Invitrogen) using the following primers: first-round PCR: forward, 5'-AAATCTTAGCAGTGGCGCCGAACAG-3'; reverse, 5'-TAACCCTGCGGGATGTGGTATTCC-3'; second-round PCR: forward, 5'-GCGCCGAACAGGGACACTGAAARCGAAAG-3'; reverse, 5'-TATCATCTGCTCCTGTATC-3'. The  $\Psi$  samples were sequenced as described for *env*. Supplementary Table 2 reports the participant HIV-1 sequences within these 3dPCR primer and probe regions, along with the sequence of any autologous oligonucleotides that were designed to accommodate HIV-1 polymorphism in 3dPCR. For participants with a polymorphism at critical residue(s), we designed custom primers and probes that matched their autologous sequence exactly. Polymorphisms at critical residues observed at a within-host frequency of less than 10% were not incorporated into the autologous primer–probe design.

Briefly, CD4<sup>+</sup> T lymphocytes were isolated from PBMCs by negative selection (CD4<sup>+</sup> T cell isolation kit, Miltenyi) and genomic DNA was extracted (DNeasy Blood and Tissue kit, Qiagen). To quantify proviruses, DNA extracts were assayed with either the published or autologous HIV-1 primer–probe sets, as described in Supplementary Table 2. In parallel, all DNA extracts were also assayed in a separate duplexed ddPCR reaction targeting the human *RPP30* gene<sup>41</sup>, using the following primers and probes: *RPP30* forward primer, 5'-GATTTGGACCTGCGAGCG-3'; *RPP30* probe, 5'-VIC-CTGACCTGAAGGCTCT-MBBNFQ-3'; *RPP30* reverse primer, 5'-GCGGCTGTCTCCACAAGT-3'; *RPP30* shear forward primer, 5'-CCATTTGCTGCTCCTTGGG-3'; *RPP30* shear probe, 5'-FAM-AAGGAGCAAGGTTCTATGTAG-MGBNFQ-3'; *RPP30* shear reverse primer, 5'-CATGCAAAGGAGGAAGCCG-3'. HIV-1 and human *RPP30* copies were then normalized to the quantity of input DNA to estimate intact HIV-1 copies per  $10^6$  CD4<sup>+</sup> T cells. Each ddPCR reaction contained genomic DNA, ddPCR Supermix for Probes (no dUTPs; Bio-Rad), primers (final concentration 900 nM; Integrated DNA Technologies), probes (final concentration 250 nM; ThermoFisher Scientific), XhoI restriction enzyme and nuclease-free water. Droplets were prepared using a QX200 Droplet Generator (Bio-Rad) and cycled at 95 °C for 10 min; 45 cycles of (94 °C for 30 s, 59 °C for 1 min) and 98 °C for 10 min, using a ramp rate of 2 °C to improve droplet separation. Droplets were analyzed on a QX200 Droplet Reader (Bio-Rad) using QuantaSoft software (Bio-Rad, version 1.7.4), where replicate wells were merged before analysis. Intact HIV-1 copies ( $\Psi$  and *env* double-positive droplets) were corrected for DNA shearing based on the frequency of *RPP30* and *RPP30* shear double-positive droplets. The median (IQR) DNA shearing index, measuring the proportion of sheared DNA in a sample, was 0.34 (0.32–0.39), comparable to that reported in the original development of the IPDA. Using the 3dPCR assay, we measured the frequencies of double-positive HIV-1 proviruses (intact) and 5'- and 3'-defective HIV-1 proviruses at baseline (day 0) and at days 180 and 365 after ART initiation. At baseline, the level of intact proviruses correlated with the frequency of induced p24<sup>+</sup> CD4<sup>+</sup> T cells, plasma HIV-1 RNA level and CD4<sup>+</sup> T cell count (Supplementary Fig. 1c–e).

Intact proviruses were also quantified by the IPDA<sup>40</sup> for 23 participants for whom sufficient sample was available at either the

day 180 ( $n = 4$ ) or day 365 ( $n = 19$ ) time point. Reactions were prepared and analysis was performed as described above for 3dPCR. Primers and probes targeting HIV-1 were as follows: HIV-1  $\Psi$  forward primer, 5'-CAGGACTCGGCTTGCTGAAG-3'; HIV-1  $\Psi$  probe, 5'-FAM-TTTGGCCGTACTCACCAGT-MGBNFQ-3'; HIV-1  $\Psi$  reverse primer, 5'-GCACCATCTCTCCTCTAGC-3'; HIV-1 *env* forward primer, 5'-AGTGGTGCAGAGAAAAAGAGC-3'; HIV-1 *env* probe, 5'-VICCCTGGGTTCTTGGGA-MGBNFQ-3'; antihypermutant *env* probe, 5'-CCTTAGGTTCTTAGGAGC-MGBNFQ-3'; HIV-1 *env* reverse primer, 5'-GTCTGGCCTGTACCGTCAGC-3'. Supplementary Table 3 reports the sequence of these participants in the IPDA  $\Psi$  and *env* regions.

The levels of intact proviruses measured by IPDA and 3dPCR correlated strongly in individuals with HIV-1 subtype B whose reservoirs could be measured using the former (six participants could not be measured by IPDA due to polymorphisms that caused signal failure). The frequency of intact proviruses as measured by 3dPCR was also comparable between individuals with HIV-1 B versus non-B subtypes. This together suggests that 3dPCR provides a reasonable estimate of intact HIV-1 reservoir size, although it is possible that the assay's positive predictive value for intact proviruses may, as in the IPDA, vary between individuals<sup>69</sup>.

### HIV antigen-producing cells using the VIP-SPOT assay

We measured HIV antigen-producing cells using the VIP-SPOT assay<sup>39</sup> at baseline (day 0) and 365 days after ART initiation. The measures of HIV antigen-producing cells per  $10^6$  CD4<sup>+</sup> T cells correlated with baseline plasma HIV-1 RNA and intact HIV-1 proviruses (Supplementary Fig. 1b,c). Briefly, CD4<sup>+</sup> T cells were isolated from  $20 \times 10^6$  cryopreserved PBMCs by negative immunomagnetic separation using the auto-MACS Pro Separator (CD4<sup>+</sup> T Cell Isolation Kit, Miltenyi) according to the manufacturer's instructions and counted using the automated NucleoCounter NC-3000 (Chemometec, Denmark). Median viability of isolated CD4<sup>+</sup> T cells was 94% (range: 72–99%). Cell suspensions containing up to  $2 \times 10^6$  cells per ml of purified CD4<sup>+</sup> T cells were prepared in culture medium and distributed in 150  $\mu$ l per well, such that  $3 \times 10^5$  cells per well were seeded in the precoated ELISpot plates. In all VIP-SPOT assays, CD4<sup>+</sup> T cells from individuals without HIV-1 were included as a negative control using PBMCs isolated from the buffy coats. The buffy coats were purchased from the Catalan Banc de Sang i Teixits (<http://www.bancsang.net/en/index.html>; Barcelona, Spain). Likewise, all plates included two positive-control wells containing J-Lat cells (clone 8.4) at an approximate concentration of  $10^2$  cells per well, in culture medium supplemented with 20 nM PMA and 0.5  $\mu$ g ml<sup>-1</sup> ionomycin (P1585 and I3909, Sigma-Aldrich). The VIP-SPOT assay was analyzed in accordance with the published method<sup>39</sup>. The frequency of HIV antigen-producing cells was determined based on the total number of spots detected for each sample and the number of CD4<sup>+</sup> T cells cultured.

### 3BNC117 sensitivity testing by either pheno- or genotypic assays

Post hoc 3BNC117 sensitivity analysis was performed after enrollment for participants receiving 3BNC117 using the Labcorp-Monogram Biosciences PhenoSense HIV Monoclonal Antibody Assay on plasma HIV-1 RNA viruses. 3BNC117 sensitivity was not a prespecified inclusion criterion. Sensitivity was defined in this study as a concentration of 3BNC117 required to inhibit viral replication by 90% ( $IC_{90}$ ) < 1.5  $\mu$ g ml<sup>-1</sup> and MPI observed at the highest 3BNC117 concentration tested > 98%. If the Labcorp-Monogram assay did not yield a result due to lack of or insufficient amplification or infectivity, *env* sequences obtained by single-genome amplification of plasma RNA viruses from baseline were analyzed using a genotypic prediction algorithm with a predefined threshold of 10% of resistant sequences.

**Plasma envelope sequencing.** To sequence single viral envelope copies, RNA was extracted from baseline plasma virus using the QIAamp Viral

RNA Mini Kit (Qiagen) and cDNA was synthesized with an *env*-specific primer (OFM19: 5'-GCACTCAAGGCAAGCTTTATTGAGGCTTA-3') using Superscript III Reverse Transcriptase (Invitrogen) and RNaseOUT (Invitrogen) with the following thermal cycling conditions: 50 °C for 1 h, 55 °C for 1 h and 70 °C for 15 min. The cDNA was diluted for nested PCR to obtain single-genome amplification (<30% of wells containing envelope). The PCR reactions were performed in 10  $\mu$ l using Platinum Taq DNA polymerase High Fidelity (Invitrogen). In the first PCR, the following primers were used: OFM19: 5'-GCACTCAAGGCAAGCTTTATTGAGGCTTA-3' and VIF1: 5'-GGGTTTATTACAGGGACAGCAGAG-3'; for the second PCR, the ENV A: 5'-GGCTTAGGCATCTCCTATGGCAGGAAGAA-3' and ENV N: 5'-CTGCCAATCAGGGAAGTAGCCTTGTGT-3' primers were used. Envelope-positive wells were determined by using E-gel (Invitrogen) and collected on a 384-well plate. The concentration was measured for representative wells, and all samples were diluted to approximately 20 ng  $\mu$ L<sup>-1</sup>. For library preparation, the samples were first subjected to tagmentation as follows: 1  $\mu$ l DNA 1.25  $\mu$ l Tagment DNA Buffer and 0.25  $\mu$ l TDE1 Tagment DNA enzyme (Illumina). Then, unique i5/i7 bar-coded primers were ligated to the tagmented DNA with the use of KAPA HIFI Hotstart ReadyMix (Roche). The barcoded amplicons were first pooled into eight Eppendorf tubes and purified with AMPure XP Beads (Beckman Coulter) and then pooled together in one library. The library was paired-end sequenced on a MiniSeq (Illumina) with the MiniSeq Mid Output kit (300 cycles).

**HIV-1 sequence assembly and annotation.** HIV-1 sequence assembly was performed by The Rockefeller University pipeline (Defective and Intact HIV Genome Assembler), which is capable of reconstructing thousands of HIV genomes within hours via the assembly of raw sequencing reads into annotated HIV genomes. The steps executed by the pipeline were as follows. First, we removed PCR amplification and performed error correction using clumpify.sh from BBtools package v38.72 (<https://sourceforge.net/projects/bbmap/>). A quality control check was performed with Trim Galore package v0.6.4 (<https://github.com/FelixKrueger/TrimGalore>) to trim Illumina adaptors and low-quality bases. We also used bbduk.sh from the BBtools package to remove possible contaminant reads using HIV genome sequences, obtained from the Los Alamos HIV database, as a positive control. Paired-overlapping reads were exported into a single read by BBMerge. We used a *k*-mer-based assembler, SPAdes v3.13.1, to reconstruct the HIV-1 sequences. The longest assembled contig was aligned via BLAST with HXB2, to set it in the correct orientation. Finally, the HIV genome sequence was annotated by aligning against HXB2 using BLAST. Sequences with double peaks, that is, regions indicating the presence of two or more viruses in the sample (cutoff consensus identity for any residue <70%), or samples with a limited number of reads (empty wells with  $\leq 500$  sequencing reads) were omitted from downstream analyses. In the end, sequences were classified as intact or defective.

**Sequence-based assessment of 3BNC117 sensitivity.** Analysis of HIV-1 *env* variants that have been described to correlate with resistance to 3BNC117 was performed in the obtained sequences by a post hoc model based on the sequencing and neutralization data to predict virus sensitivity. Based on the published data, the following amino acid rules (using HXB2 numbering) were used to determine 3BNC117-sensitive strains: 15N or D at 279, not K or D at 280, R at 456, D at 457, G at 458, G at 459, no PNGS at 279 (not N279 and S or T at 281).

All viral sequences have been deposited in GenBank with accession numbers ON542594 to ON542710 ([www.ncbi.nlm.nih.gov/nucleotide/](http://www.ncbi.nlm.nih.gov/nucleotide/)).

### HLA class I typing

HLA class I (HLA-A, HLA-B, HLA-C) alleles were genotyped at the American Safety and Health Institute-accredited laboratory HistoGenetics (Ossining, NY, USA) using sequence-based typing.

### Asanté recency testing

Recency testing was performed on plasma obtained at baseline using the Asanté HIV-1 Rapid Recency Assay (Sedia Biosciences Corporation) according to the manufacturer's protocol<sup>70</sup>.

### Twelve-week ATI

Enrollment into the 12-week ATI was optional and conditioned by the following criteria on the individual level:

1. Undetectable plasma HIV-1 RNA levels of <50 copies per ml during the last 6 months (one 'viral blip' >50 copies per ml was acceptable)
2. Latest CD4<sup>+</sup> T cell count of >500 cells per mm<sup>3</sup>

The following criteria were used to restart ART:

1. Two consecutive plasma HIV-1 RNA measurements of >5,000 copies per ml
2. CD4<sup>+</sup> T cell count of <350 cells per mm<sup>3</sup>
3. Participant request
4. If ART interruption in the opinion of the sponsor or investigator contained an unacceptable risk to the participant

### Outcomes

The primary endpoints were as follows: (1) viral decay kinetics after ART initiation using plasma HIV-1 levels and (2) changes in reservoir size measured by double-positive HIV-1 proviruses and HIV antigen-producing cells per 10<sup>6</sup> unfractionated CD4<sup>+</sup> T cells. Secondary endpoints were as follows: (1) safety including CD4<sup>+</sup> T cell counts; (2) changes in the transcriptionally and/or translationally active HIV-1-infected cells during the first 30 days of ART using FISH-flow assay; (3) effects on HIV-1 Gag-specific T cell immunity using the AIM assay; (4) time to loss of virologic control during the ATI (we defined loss of virologic control as two consecutive plasma HIV-1 RNA measurements of ≥5,000 copies per ml; if CD4<sup>+</sup> T cell counts decreased to <350 cells per mm<sup>3</sup>, ART was also resumed<sup>71</sup>); and (5) posthoc baseline (day 0) sensitivity to 3BNC117 and recency testing.

### Statistical methods

At the time of protocol development, there was no validated PCR assay for estimating the size of the intact proviral reservoir, so the sample size was based on anticipated changes in total HIV-1 DNA. The anticipated average individual change in total HIV-1 DNA was approximately -0.85 per 10<sup>6</sup> CD4<sup>+</sup> T cells on the log<sub>10</sub> scale with corresponding s.d. of 0.35 from baseline (time of ART initiation) to 365 days after ART initiation, when not receiving 3BNC117 or RMD<sup>72</sup>. One of the primary endpoints was change in total HIV-1 DNA from baseline to 365 days after ART initiation in the ART + 3BNC117 + RMD group compared to the ART-only group. The ART + 3BNC117 and ART + RMD groups were used to compare secondary endpoints in terms of the specific effects of each of the interventions alone, but the trial was powered according to the decline in total HIV-1 DNA in the ART-only and ART + 3BNC117 + RMD groups:  $\delta$ ART and  $\delta$ ART + 3BNC117 + RMD. Based on a two-sample mean comparison under the null hypothesis  $H_0$ :  $\delta$ ART =  $\delta$ ART + 3BNC117 + RMD, the expected values of -0.85 and -1.35, respectively, and an s.d. of 0.35, a power of 90% is achieved with enrollment of 12 participants in each arm at a 5% significance level. To accommodate dropouts, we aimed for 15 participants in each arm. We considered a two-sided  $\alpha$  value of less than 0.05 significant. We later used the 3dPCR assay based on the IPDA protocol and adopted this as our primary reservoir measurement as we believe that the 3dPCR assay is superior to total HIV-1 DNA in terms of estimating the intact HIV-1 reservoir. Protocol amendments did not affect the analysis plan besides the reservoir size analyses described above. The analyses performed on primary and secondary endpoints were prespecified

in the protocol, and no exploratory analyses were done; hence, no corrections for multiple comparisons were made.

We used multiple imputation to impute missing values in plasma HIV-1 RNA. Such missing values could occur due to a measurement not being conducted or being below the LQ ( <20 copies per ml). After natural log transformation of the plasma HIV-1 RNA levels, we used linear regression in the imputation model for absent measurements and interval regression for measurements below the quantification limit. As predictors in the regression models, we used the previous and subsequent measurements. Using interval regression together with multiple imputation is a standard approach for handling interval-censored data, including in situations with censoring due to a quantification limit. The method also handles missing values by interval censoring<sup>73</sup>. In brief, based on the observed and (interval) censored values, the method estimates how the mean of natural log-transformed plasma HIV-1 RNA depends on a linear function of covariates, assuming that the outcomes follow a normal distribution with an unknown but constant variance. This model is completely similar to ordinary linear regression, although observations may now be intervals instead of specific values. Once the mean function and variance were estimated, imputation values for the missing data were generated from a truncated normal distribution for the interval-censored observations using standard random number generation techniques. To achieve good asymptotic properties of estimates, we imputed 100 datasets. The analysis of multiply imputed datasets was done via Rubin's formula, which states that analyses of each imputed dataset may be validly joined into a single combined estimate<sup>74,75</sup>. Mixed-effects linear regression models with a random effect for individual participants were used to analyze decay rates between groups. Paired two-tailed Wilcoxon tests and two-tailed Mann-Whitney tests were used to analyze nonparametric outcomes within and between groups, respectively. When more than two groups were compared using nonparametric statistics, the Kruskal-Wallis test was used. Paired and unpaired *t*-tests were used to analyze parametric outcomes within and between groups, respectively. Fisher's exact test was used to analyze contingency tables. Data are presented as median (IQR), median (range) or mean  $\pm$  s.d. as indicated in each respective figure legend. The Kaplan-Meier estimator was used to assess the magnitude of the difference between the survival curves, and the log-rank test was used to compare time to loss of virologic control during the ATI between groups. For correlations, Spearman's correlation coefficient was used. We used the full analysis set, comprising all individuals receiving at least one dose of active treatment with assessable data, for the efficacy analyses and all enrolled individuals for the safety analyses. We used Stata version 17.0 and Prism version 7.0 for statistical analyses.

### Reporting summary

Further information on research design is available in the Nature Research Reporting Summary linked to this article.

### Data availability

Data are not available for download due to privacy/ethical restrictions under the EU GDPR. Specific requests for access to the trial data may be sent to [olesoega@rm.dk](mailto:olesoega@rm.dk) and access may be provided to a named individual in agreement with the rules and regulations of the Danish Data Protection Agency and the National Committee on Health Research Ethics with a 2-week response timeframe to requests.

### References

64. Schulz, K. F., Altman, D. G. & Moher, D. CONSORT 2010 statement: updated guidelines for reporting parallel group randomised trials. *Trials* **11**, 32 (2010).
65. Harris, P. A. et al. Research electronic data capture (REDCap)—a metadata-driven methodology and workflow process for providing translational research informatics support. *J. Biomed. Inform.* **42**, 377–381 (2009).



66. Harris, P. A. et al. The REDCap consortium: building an international community of software platform partners. *J. Biomed. Inform.* **95**, 103208 (2019).
67. Baxter, A. E. et al. Single-cell characterization of viral translation-competent reservoirs in HIV-infected individuals. *Cell Host Microbe* **20**, 368–380 (2016).
68. Grau-Expósito, J. et al. A novel single-cell FISH-flow assay identifies effector memory CD4<sup>+</sup> T cells as a major niche for HIV-1 transcription in HIV-infected patients. *mBio* **8**, e00876-17 (2017).
69. Gaebler, C. et al. Combination of quadruplex qPCR and next-generation sequencing for qualitative and quantitative analysis of the HIV-1 latent reservoir. *J. Exp. Med.* **216**, 2253–2264 (2019).
70. Parekh, B. S. et al. *Performance evaluation of Asante rapid recency assay for HIV diagnosis and detection of recent infection: potential for surveillance and prevention*. In: *Ninth IAS Conference on HIV Science* (2017).
71. Julg, B. et al. Recommendations for analytical antiretroviral treatment interruptions in HIV research trials—report of a consensus meeting. *Lancet HIV* **6**, e259–e268 (2019).
72. Besson, G. J. et al. HIV-1 DNA decay dynamics in blood during more than a decade of suppressive antiretroviral therapy. *Clin. Infect. Dis.* **59**, 1312–1321 (2014).
73. Royston, P. Multiple imputation of missing values: further update of ice, with an emphasis on categorical variables. *Stata J.* **9**, 466–477 (2009).
74. Rubin D. B. *Multiple Imputation for Nonresponse in Surveys* (Wiley, 2004).
75. Austin, P. C., White, I. R., Lee, D. S. & van Buuren, S. Missing data in clinical research: a tutorial on multiple imputation. *Can. J. Cardiol.* **37**, 1322–1331 (2021).

## Acknowledgements

We thank all study participants who devoted time to our research as well as every clinical research unit involved in the study: at Aarhus University Hospital—study nurses Yordanos Yehdego, Ane Søndergaard and Ann Bach, physicians Janne T. Martinsen and Nina B. Stærke and lab technician Lene S. Jøhnke; at Copenhagen University Hospital—Amager and Hvidovre—study nurses Dorthe K. Petersen and Louise Krohn-Dehli and lab technician Anna L. Sørensen; at Aalborg University Hospital—study nurses Maria R. Juhl and Kristine T. Pedersen; at Odense University Hospital—study nurses Susan O. Lindvig and Bente Ramskov; at Regional Hospital Herning—study nurses Kirsten Lillevang and Heidi G. Sørensen; at Imperial College Hospital—study nurses Rebecca Hall, Claire Petersen and Shelly Page, physician John Thornhill, lab technician Andrew O Lovell and study coordinator Tom Cole; at King's College London—study nurses Anele Waters, Rebekah Roberts, Hiromi Uzu and Andrea Berlanga and study coordinator Alice Sharp; and at the Danish Good Clinical Practice Units—monitors Lene Brandsborg, Inge M. Burmeister and Stine K. Hovgaard. We acknowledge Rockefeller University for providing 3BNC117 and Bristol-Myers Squibb Company (Celgene Corporation) for providing the RMD as well as the Labcorp-Monogram Biosciences Clinical Reference Laboratory for performing the phenotypic resistance assays with project management from Y. Lie and C. Kang. Finally, we would like to acknowledge the amazing support and help from the late Amin Alamshah, a kind and brilliant clinical project manager at the Imperial College Center for Translational

and Experimental Medicine, who tragically lost his life before the completion of this study. The funders were not involved in the study design/operations, data collection/analysis/interpretation or preparation of the manuscript. This study is funded by the Danish Council for Independent Research (grant numbers: 7016-00022 and 9060-00023B to O.S.S.), the Central Region Denmark Research Fund, The Danish Regions' Medicine and Treatment Fund, Aarhus University and Next Experimental Therapy Partnership. Research reported in this publication was also supported by the National Institute of Allergy and Infectious Diseases of the National Institutes of Health (award number: UM1AI164565 to R.B.J.). The content is solely the responsibility of the authors and does not necessarily represent the official views of the National Institutes of Health. N.N.K. received a Vanier Award from the Canadian Institutes for Health Research. Z.L.B. received a scholar award from the Michael Smith Foundation for Health Research. Study drugs were donated free of charge by The Rockefeller University (3BNC117) and Celgene (romidepsin) for use in this trial. None of the specific sources of funding had any role in the conceptualization, design, data collection, analysis, decision to publish or preparation of the manuscript.

## Author contributions

O.S.S. developed the trial design. J.D.G., M.T., M.C.N., M.C. and O.S.S. wrote the protocol. J.D.G., T.B., H.N., I.S.J., R.M., L.Ø., V.K., J.F., S.F. and O.S.S. did the clinical visits. J.D.G., M.H.P., M.R.-U., I.-N.L., M.K., M.H.S., R.O., P.W.D., N.N.K., D.C.C., A.R.W., W.D.C.A., S.D.N., M.C.P., J.D.R., C.J.P., J.M.-P., Z.L.B., R.B.J., M.T. and O.S.S. did the laboratory assays and validations. V.R. performed the bioinformatic analysis. J.D.G., M.H.P., M.R.-U. and H.S. did the statistical analysis. J.D.G., P.W.D. and O.S.S. drafted the tables and figures. J.D.G. and O.S.S. drafted the article, which all authors critically revised for important intellectual content. J.D.G. and O.S.S. had full access to all the data in the study, verified the data and had final responsibility for the decision to submit for publication.

## Competing interests

M.C.N. is listed as an inventor on patents for the antibody 3BNC117. J.D.R. and C.J.P. are employees of Labcorp-Monogram Biosciences. All other authors declare no competing interests.

## Additional information

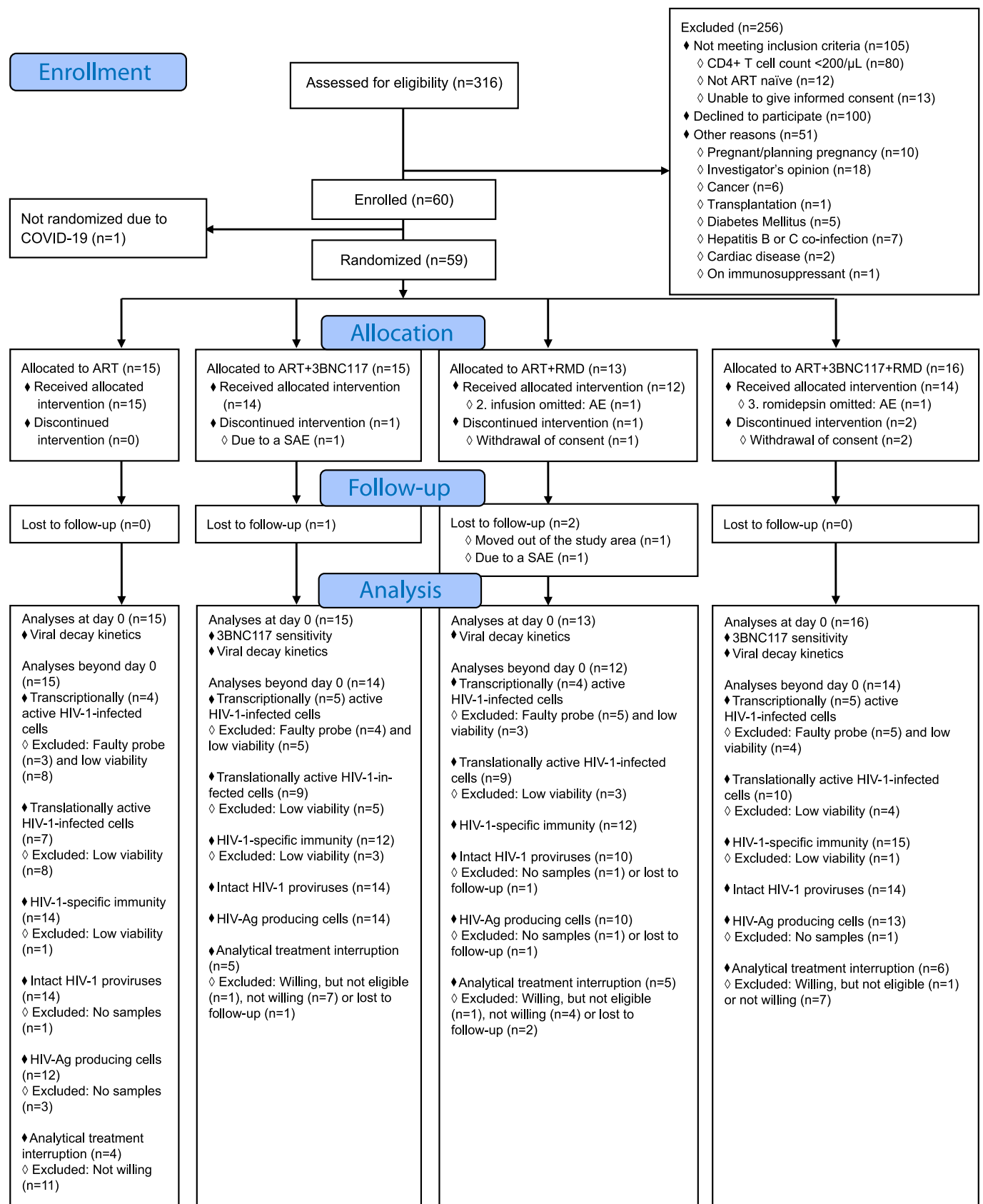
**Extended data** is available for this paper at <https://doi.org/10.1038/s41591-022-02023-7>.

**Supplementary information** The online version contains supplementary material available at <https://doi.org/10.1038/s41591-022-02023-7>.

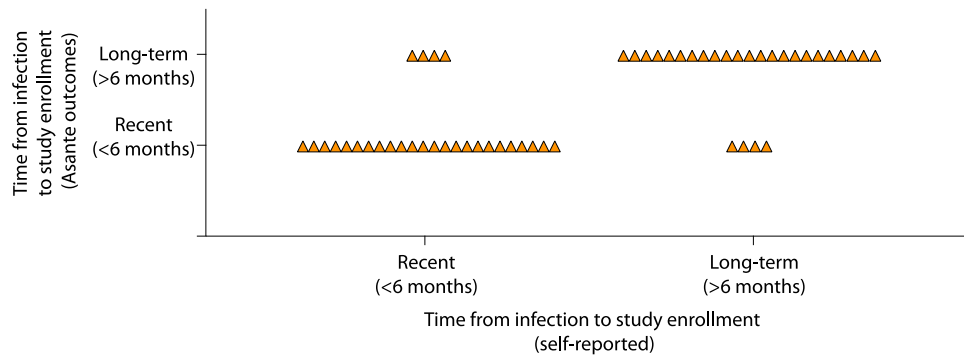
**Correspondence and requests for materials** should be addressed to Ole S. Søgaard.

**Peer review information** *Nature Medicine* thanks the anonymous reviewers for their contribution to the peer review of this work. Primary Handling Editor: Alison Farrell, in collaboration with the *Nature Medicine* team.

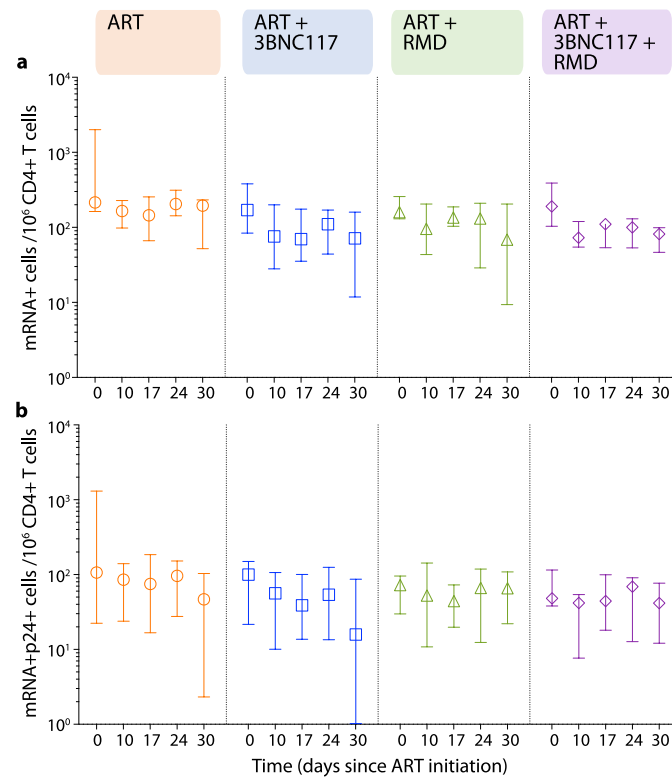
**Reprints and permissions information** is available at [www.nature.com/reprints](http://www.nature.com/reprints).



**Extended Data Fig. 1 | A comprehensive CONSORT Flow Diagram.** AE, adverse event; Ag, antigen; ART, antiretroviral therapy; COVID-19, coronavirus disease 2019; RMD, romidepsin; SAE, serious AE.

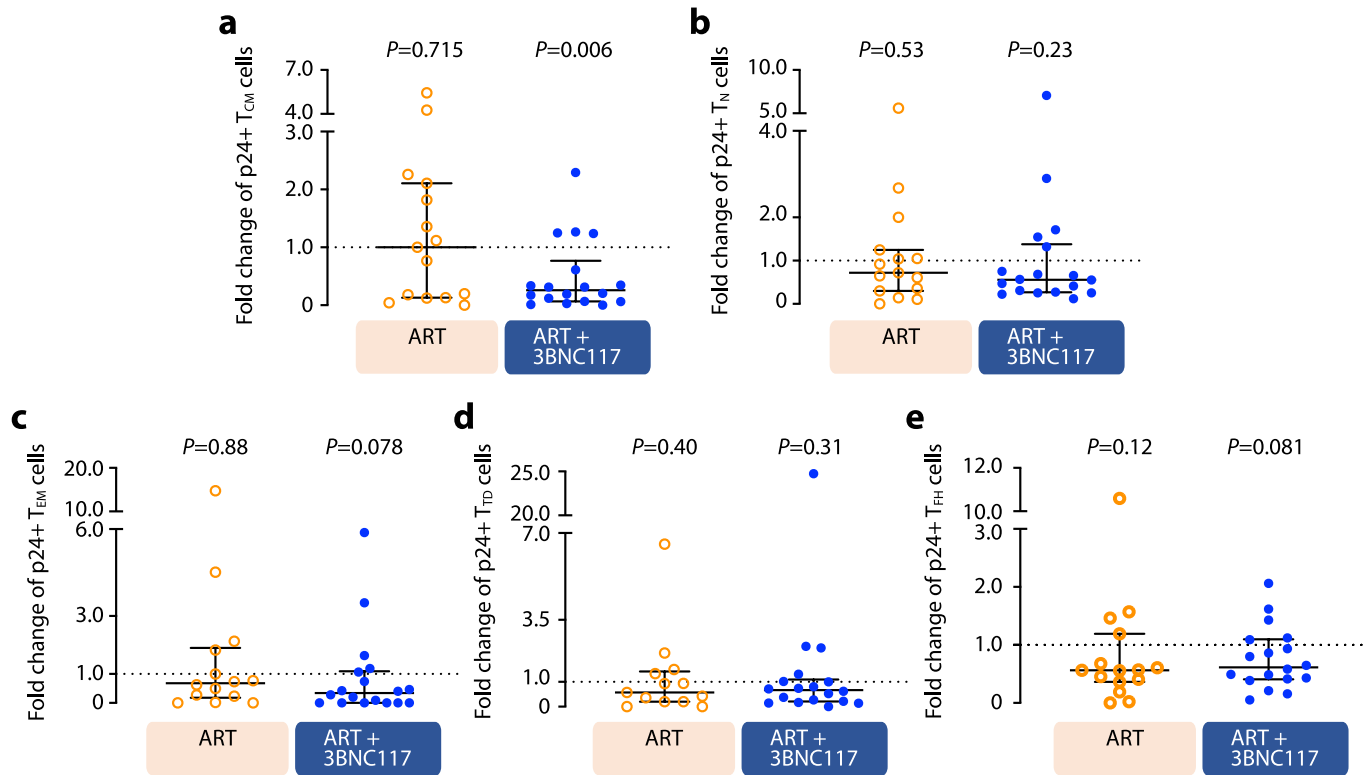


**Extended Data Fig. 2 | Distribution between self-report time of infection to study enrollment and outcome of the Asanté HIV-1 Rapid Recency Assay (n = 54).**



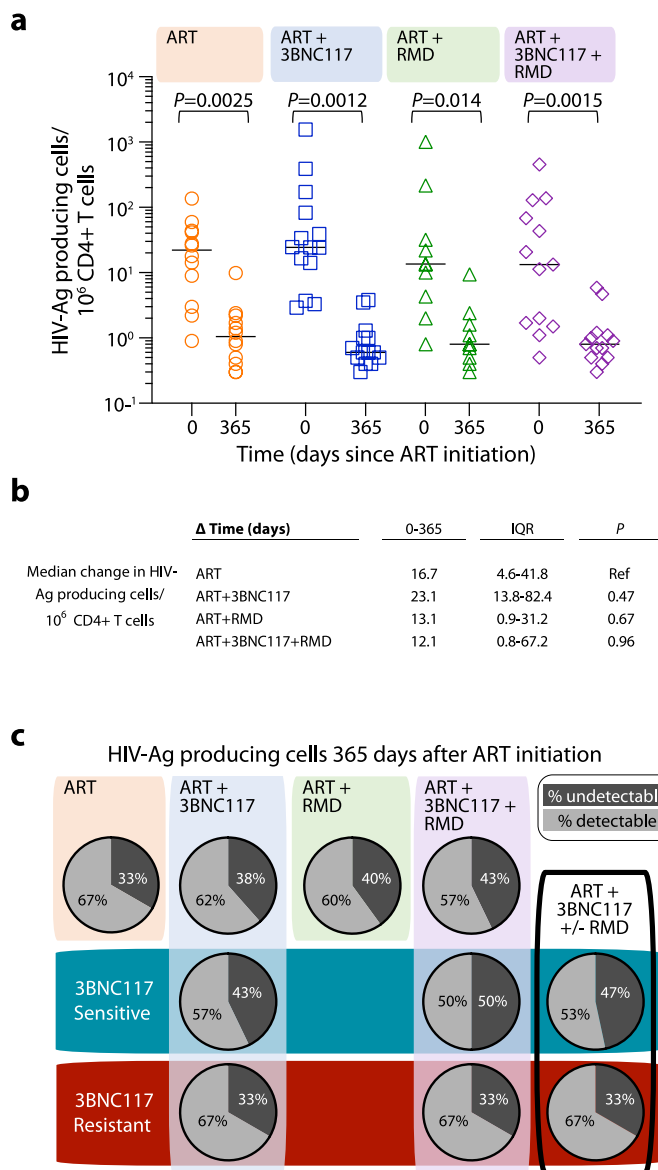
**Extended Data Fig. 3 | Transcriptionally (mRNA+) and transcriptionally + translationally (mRNA+p24+) active HIV-1-infected cells following ART initiation.** Changes in HIV-1-infected cells during the first 30 days of ART among the four groups shown as median (error bars represents interquartile ranges)

number of CD3+CD8- T cells expressing either HIV-1 mRNA (a) or HIV-1 mRNA and Gag p24 protein (b). ART-control n = 4, ART + 3BNC117 n = 5, ART + RMD n = 4, ART + 3BNC117 + RMD n = 5. ART, antiretroviral therapy; RMD, romidepsin.



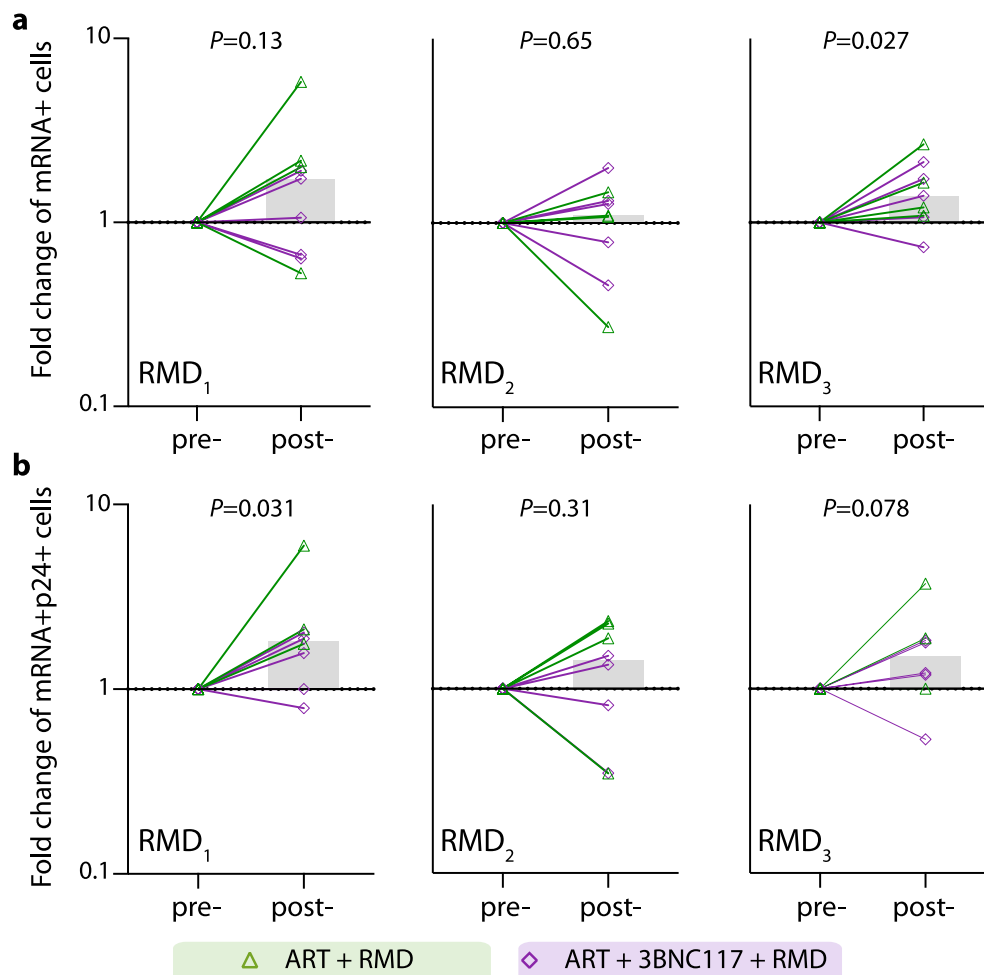
**Extended Data Fig. 4 | Impact of 3BNC117 on translationally (p24+) active HIV-1-infected CD4+ T cell subsets.** Data are shown as in Fig. 3b-e, where the ART alone and ART + RMD groups (who only received ART during the first 10 days) are combined into one group and compared to the two 3BNC117-treated groups. Median (error bars represent interquartile ranges) fold change in CD3+CD8- T cell subsets expressing Gag p24 among the combined ART (n = 15)

and ART + 3BNC117 (n = 18) groups. The CD3+CD8- T cells subsets are central memory T cells ( $T_{CM}$ ) (a), naive T cells ( $T_N$ ) (b), effector memory T cells ( $T_{EM}$ ) (c), terminally differentiated T cells ( $T_{TD}$ ) (d), and T follicular helper cells ( $T_{FH}$ ) (e). *P* values comparing within group was calculated using paired two-tailed Wilcoxon test. ART, antiretroviral therapy; IQR, interquartile ranges; RMD, romidepsin.



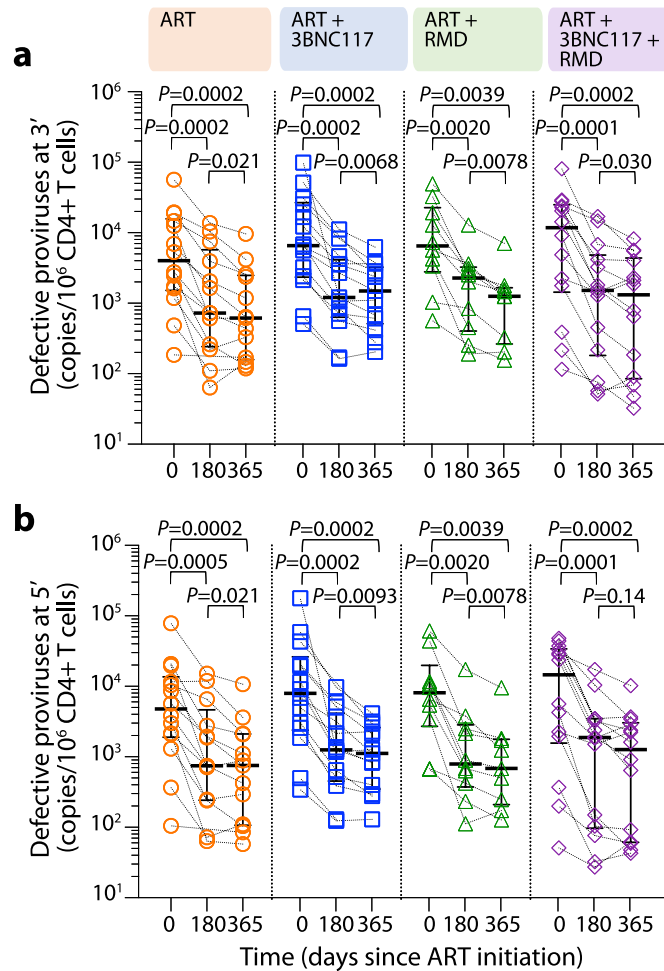
**Extended Data Fig. 5 | The frequency of HIV-1 antigen-producing cells.** The individual frequency of induced p24+ CD4+ T cells at ART initiation (day 0) and after 365 days of ART (lines at median) (a) and median changes in these cells between day 0 and 365 after ART initiation (b) among individuals in the four groups. P values comparing within group and between groups were calculated using paired two-tailed Wilcoxon test and two-tailed Mann-Whitney test, respectively. Pie charts showing the status of HIV-1 antigen-producing

cells after 365 days of ART per group (column and upper row) and categorized according to pre-ART plasma virus sensitivity (middle row; blue shaded area) or resistance (bottom row; red shaded area) to 3BNC117 (c). A compiled group ART + 3BNC117 +/- RMD is shown in the last column. ART-control n = 12, ART + 3BNC117 n = 14, ART + RMD n = 10, ART + 3BNC117 + RMD n = 13. Ag, antigen; ART, antiretroviral therapy; RMD, romidepsin.



**Extended Data Fig. 6 | Effect of RMD on transcriptionally (mRNA+) and transcriptionally + translationally (mRNA+p24+) active HIV-1-infected cells.** Data are shown as in Fig. 3f, g. Individual and overall median fold change (column) from pre- to post-RMD infusions in groups ART + RMD (n = 8) and ART + 3BNC117 + RMD (n = 10) on CD3+CD8- T cells expressing HIV-1 mRNA (a)

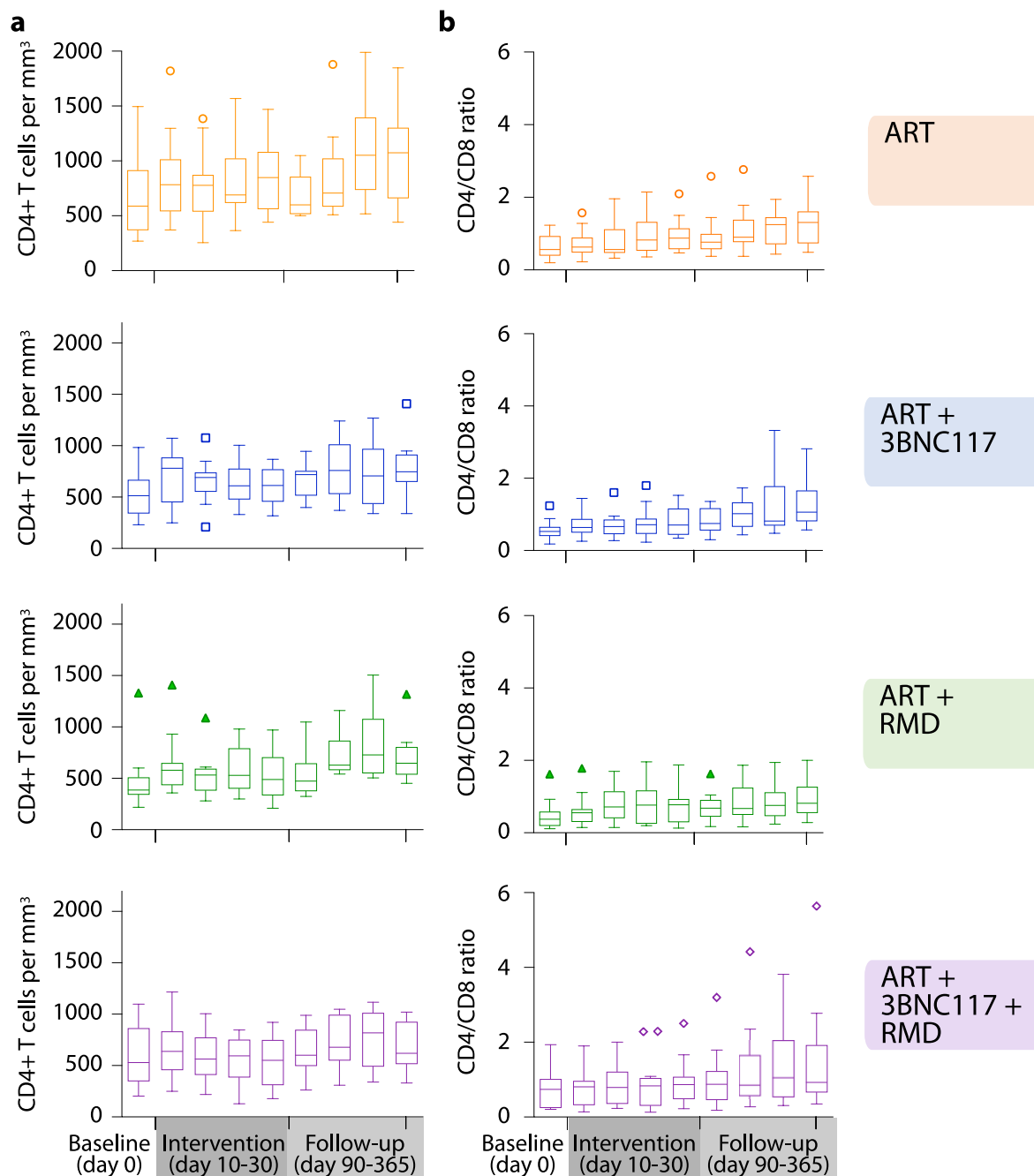
or mRNA and Gag p24 (b). *P* values comparing within group was calculated using paired two-tailed Wilcoxon test. Due to a faulty mRNA probe in the 2<sup>nd</sup> batch of FISH-flow cytometry analyses, mRNA data was only available for half of the study population. ART, antiretroviral therapy; RMD, romidepsin.



**Extended Data Fig. 7 | The frequency of defective HIV-1 proviruses.** The frequency of 3' (a) and 5' (b) defective HIV-1 proviruses at ART initiation and after 180 and 365 days of ART among individuals in the four groups (lines at median, error bars represent interquartile ranges). *P* values comparing within group were

calculated using paired two-tailed Wilcoxon test. ART only n = 14, ART + 3BNC117 n = 14, ART + RMD n = 10, ART + 3BNC117 + RMD n = 14. ART, antiretroviral therapy; RMD, romidepsin.





**Extended Data Fig. 8 | CD4+ T cell count and CD4/CD8 ratio during the study.** Tukey plots depicts the CD4+ T cell count (a) and CD4/CD8 ratio (b) in the four groups at baseline (day 0), the interventional period (day 10–30) and during follow-up (day 90–365). Lines indicates median, boxes represent

interquartile ranges and whiskers drawn within the 1.5 IQR values. ART only n = 15, ART + 3BNC117 n = 15, ART + RMD n = 13, ART + 3BNC117 + RMD n = 16. ART, antiretroviral therapy; IQR, interquartile range; RMD, romidepsin.

Extended Data Table 1 | Individual baseline characteristics for the study population

	HIV-1 subtype	HLA class I alleles						Plasma HIV-1 RNA (copies/mL)	CD4+ T cells (per mm <sup>3</sup> )	ART regimen	Intact HIV-1 proviruses (copies/10 <sup>6</sup> CD4+ T cells)	
		A1	A2	B1	B2	C1	C2					
ART-control (n=15)	105	C	02:01:01G	24:02:01G	08:01:01G	15:01:01G	03:03:01G	07:01:01G	290,000	NA	ABA 3TC, DTG	81,027.8
	110	D	01:01:01G	29:02:01G	08:01:01G	44:03:01G	07:01:01G	16:01:01G	88,000	1,440	TDF, 3TC, DTG	11,479.5
	120	B	02:03:01	02:03:01	46:01:01	51:01:02	01:02:01G	14:02:01G	15,500	560	FTC, 3TC, DTG	12,443.0
	201	C	01:01:01G	23:01:01G	08:01:01G	44:03:01G	04:01:01G	07:01:01G	3,240,000	344	ABA 3TC, DTG	3,927.7
	206	CRF01	01:01:01G	02:01:01G	37:01:01G	44:02:01G	06:02:01G	07:04:01G	78,300	271	FTC, 3TC, DTG	2,516.9
	208	CRF other	02:02:01G	02:01:01G	14:02:01G	58:02:01G	06:02:01G	08:02:01G	31,800	NA	ABA 3TC, DTG	2,813.5
	209	B	03:01:01G	30:04:01G	14:02:01G	40:02:01G	02:02:02G	08:02:01G	16,900	948	TDF, 3TC, DTG	1,144.6
	305	B	03:01:01G	03:01:01G	07:02:01G	35:01:01G	04:01:01G	07:02:01G	6,415	590	TDF, FTC, DTG	304.3
	306	B	11:01:01G	24:02:01G	18:01:01G	35:03:01G	04:01:01G	07:01:01G	4,194	710	TDF, FTC, DTG	926.2
	405	F	03:01:01G	03:01:01G	35:03:01G	44:02:01G	04:01:01G	07:04:01G	499,000	765	TDF, FTC, DTG	1,327.7
	407	B	23:01:01G	26:01:01G	49:01:01G	53:01:01G	04:01:01G	07:01:01G	29,200	394	ABA 3TC, DTG	NA
	409	B	01:01:01G	68:02:01G	14:02:01G	57:01:01G	07:01:01G	08:02:01G	39,207	466	TDF, FTC, DTG	4,052.8
	410	B	02:01:01G	24:02:01G	07:02:01G	15:01:01G	03:03:01G	07:02:01G	128,052	886	TDF, FTC, DTG	13,254.8
	702	D	29:02:01G	66:01:01G	18:01:01G	35:01:01G	04:01:01G	05:01:01G	110,000	338	ABA 3TC, DTG	14,043.8
	707	CRF01	02:01:01G	02:01:01G	57:01:01G	51:01:01G	06:02:01G	06:02:01G	820	1,497	TDF, FTC, DTG	162.0
ART+3BNC117 (n=15)	106	CRF01	26:01:01G	68:01:02G	07:02:01G	40:01:01G	03:04:01G	07:02:01G	681,000	230	TDF, 3TC, DTG	NA
	109	D	11:01:01G	24:02:01G	07:02:01G	39:01:01G	07:02:01G	07:02:01G	22,400	660	TDF, FTC, DTG	394.4
	125	B	23:01:01G	26:01:01G	08:01:01G	40:01:01G	03:04:01G	07:01:01G	42,700	290	ABA 3TC, DTG	6,172.8
	126	CRF01	02:06:01G	11:01:01G	15:21:01G	38:02:01G	04:03:01G	07:02:01G	71,900	320	ABA 3TC, DTG	81,795.7
	135	CRF01	24:07:01G	33:03:07	15:01:01G	44:03:02G	04:01:01G	07:01:01G	33,800	NA	TDF, FTC, DTG	1,817.3
	205	B	01:01:01G	02:01:01G	08:01:01G	37:01:01G	06:02:01G	07:01:01G	413,000	984	ABA 3TC, DTG	4,908.5
	210	B	01:01:01G	24:02:01G	08:01:01G	39:06:02G	07:02:01G	07:01:01G	100,000	700	ABA 3TC, DTG	1,384.4
	211	B	11:01:01G	11:01:01G	18:01:01G	51:01:01G	07:01:01G	15:13:01	65,700	414	TDF, FTC, DTG	8,776.8
	302	CRF01	01:01:01G	03:01:01G	14:02:01G	37:01:01G	06:02:01G	08:02:01G	37,726	760	TDF, FTC, DTG	31,179.2
	401	B	02:01:01G	30:02:01G	07:05:01G	44:02:01G	02:02:02G	15:05:01G	33,700	661	TDF, FTC, DTG	4,478.9
	404	A	30:01:01G	68:01:01G	50:01:01G	51:01:01G	15:02:01G	16:01:01G	16,200	457	TDF, FTC, DTG	3,003.4
	412	B	02:01:01G	23:01:01G	35:01:01G	49:01:01G	04:01:01G	07:01:01G	4,190,000	525	TAF, FTC, BIC	25,230.8
	701	B	02:01:01G	02:01:01G	15:01:01G	44:02:01G	03:03:01G	05:01:01G	740	508	ABA 3TC, DTG	351.4
	703	CRF02	01:01:01G	24:02:01G	07:02:01G	08:01:01G	07:02:01G	07:01:01G	24,000,000	345	TAF, FTC, DTG	95,783.6
	704	CRF01	01:01:01G	24:02:01G	44:02:01G	57:01:01G	05:01:01G	06:02:01G	56,800	631	TDF, FTC, DTG	30,287.2
ART+RMD (n=13)	104	B	02:01:01G	02:01:01G	15:01:01G	44:05:01G	02:02:02G	03:28	116,000	600	TDF, 3TC, DTG	601.6
	108	CRF01	11:01:01G	11:01:01G	40:01:01G	51:01:01G	07:02:01G	14:02:01G	21,061	1,333	TDF, FTC, DTG	585.0
	115	B	01:01:01G	34:01:01G	15:21:01G	27:02:01G	02:02:02G	04:03:01G	49,400	490	TDF, FTC, DTG	NA
	117	B	02:01:01G	24:02:01G	40:02:01G	56:01:01G	01:02:01G	02:02:02G	44,200	500	TDF, 3TC, DTG	134,766.0
	131	C	29:02:01G	74:01:01G	15:03:01G	42:01:01G	02:10:01G	17:01:01G	3,800	220	TDF, FTC, DTG	2,641.4
	202	B	01:01:01G	01:01:01G	07:02:01G	08:01:01G	07:02:01G	07:01:01G	141,000	354	ABA 3TC, DTG	8,091.5
	204	C	03:01:01G	29:02:01G	07:02:01G	37:01:01G	06:02:01G	07:02:01G	437,000	363	FTC, 3TC, DTG	5,580.2
	207	B	01:01:01G	03:01:01G	08:01:01G	15:01:01G	07:01:01G	15:05:01G	43,900	NA	ABA 3TC, DTG	4,270.7
	307	CRF01	01:01:01G	33:01:01G	14:02:01G	50:01:01G	06:02:01G	08:02:01G	16,466	340	TDF, FTC, DTG	10,943.0
	403	A	01:01:01G	24:02:01G	08:01:01G	58:01:01G	03:16	07:01:01G	14,600	513	ABA 3TC, DTG	5,816.7
	406	B	01:01:01G	25:01:01G	08:01:01G	18:01:01G	07:01:01G	12:03:01G	968,000	266	TDF, FTC, DTG	NA
	705	CRF01	02:01:01G	03:01:01G	07:02:01G	40:01:01G	03:04:01G	07:02:01G	110,000	348	ABA 3TC, DTG	NA
	708	CRF02	02:05:01G	24:02:01G	35:03:01G	41:01:01G	04:01:01G	17:01:01G	1,900,000	391	ABA 3TC, DTG	29,484.6
ART+3BNC117+RMD (n=16)	103	B	24:02:01G	26:01:01G	27:05:02G	38:01:01G	02:02:02G	12:03:01G	730	610	TDF, 3TC, DTG	190.5
	107	CRF01	02:01:01G	25:01:01G	15:01:01G	44:02:01G	03:03:01G	05:03:01G	188,945	470	TDF, FTC, DTG	3,144.5
	112	G	02:01:01G	68:01:02G	15:78:01	44:02:01G	03:04:01G	07:04:01G	23,100	560	TDF, 3TC, DTG	10,599.5
	116	C	01:01:01G	02:01:01G	15:01:01G	57:03:01G	03:04:01G	07:01:01G	69,400	380	ABA 3TC, DTG	212.3
	130	CRF01	02:01:01G	02:01:01G	15:01:01G	44:02:01G	03:04:01G	07:04:01G	3,710	260	TDF, 3TC, DTG	26,738.8
	203	CRF01	01:01:01G	02:01:01G	07:02:01G	08:01:01G	07:02:01G	07:01:01G	1,450,000	313	ABA 3TC, DTG	16,279.3
	212	CRF47	01:01:01G	02:01:01G	44:02:01G	57:01:01G	05:01:01G	06:02:01G	925,000	NA	TDF, FTC, DTG	18,229.7
	301	B	02:01:01G	02:01:01G	27:05:02G	44:02:01G	01:02:01G	05:01:01G	16,281	800	TDF, FTC, DTG	67,360.0
	303	CRF02	25:01:01G	68:01:02G	18:01:01G	44:02:01G	05:01:01G	07:01:01G	2,274	930	TDF, FTC, DTG	NA
	304	B	02:01:01G	02:01:01G	40:01:01G	51:01:01G	03:04:01G	15:02:01G	317,431	NA	TDF, FTC, DTG	33,443.4
	308	CRF01	02:01:01G	02:01:01G	49:01:01G	55:01:01G	03:03:01G	07:01:01G	4,180,000	NA	TDF, FTC, DTG	26,916.3
	402	B	01:01:01G	23:01:01G	14:02:01G	45:01:01G	06:02:01G	08:02:01G	18,100	950	TDF, FTC, RAL	1,001.0
	408	B	11:02:01G	24:07:01G	07:05:01G	15:02:01G	07:02:01G	08:01:01G	197,934	203	TDF, FTC, DTG	21,575.1
	411	B	01:01:01G	29:02:01G	52:01:01G	57:01:01G	04:01:01G	06:02:01G	762	1,098	TDF, FTC, DTG	40.5
	706	B	02:07:01G	11:01:01G	46:01:01G	46:01:01G	01:02:01G	01:02:01G	59,000	377	ABA 3TC, DTG	NA
	709	B	01:01:01G	02:01:01G	15:01:01G	49:01:01G	03:04:01G	07:01:01G	41,000	531	TAF, FTC, BIC	1,522.7

ABA, abacavir; ART, antiretroviral therapy; BIC, bictegravir; CRF, circulating recombinant form; DTG, dolutegravir; FTC, emtricitabine; HLA, human leukocyte antigen; NA, not available; RAL, raltegravir; RMD, romidepsin, TAF, tenofovir alafenamide; TDF, tenofovir disoproxil fumarate; 3TC, lamivudine.

Extended Data Table 2 | Adverse events

	ART group (n=15)					ART+3BNC117 group (n=15)					ART+RMD group (n=13)					ART+3BNC117+RMD group (n=16)					
	Participants		Mild	Mod.	Sev.	Participants		Mild	Mod.	Sev.	Participants		Mild	Mod.	Sev.	Participants		Mild	Mod.	Sev.	
	n	%	n	n	n	n	%	n	n	n	n	%	n	n	n	n	%	n	n	n	
<b>Events related to 3BNC117</b>																					
Any	-	-	-	-	-	6	40	-	-	-	-	-	-	-	-	7	44	-	-	-	-
Fatigue	-	-	-	-	-	4	27	4	1	-	-	-	-	-	-	3	19	5	-	-	-
Headache	-	-	-	-	-	3	20	4	-	-	-	-	-	-	-	3	19	3	-	-	-
Chills	-	-	-	-	-	1	7	1	-	-	-	-	-	-	-	2	3	2	-	-	-
Blurred vision	-	-	-	-	-	2	13	2	-	-	-	-	-	-	-	-	-	-	-	-	-
Allergic rhinitis	-	-	-	-	-	1	7	1	-	-	-	-	-	-	-	-	-	-	-	-	-
Diarrhea	-	-	-	-	-	1	7	1	-	-	-	-	-	-	-	-	-	-	-	-	-
Dizziness	-	-	-	-	-	1	7	1	-	-	-	-	-	-	-	-	-	-	-	-	-
Dysgeusia	-	-	-	-	-	1	7	1	-	-	-	-	-	-	-	-	-	-	-	-	-
Hot flashes	-	-	-	-	-	-	-	-	-	-	-	-	-	-	-	1	6	-	1	-	-
Malaise	-	-	-	-	-	1	7	1	-	-	-	-	-	-	-	-	-	-	-	-	-
Nausea	-	-	-	-	-	1	7	1	-	-	-	-	-	-	-	-	-	-	-	10	1
<b>Total</b>																					
	<b>Participants</b>		<b>Mild</b>	<b>Mod.</b>	<b>Sev.</b>	<b>Participants</b>		<b>Mild</b>	<b>Mod.</b>	<b>Sev.</b>	<b>Participants</b>		<b>Mild</b>	<b>Mod.</b>	<b>Sev.</b>	<b>Participants</b>		<b>Mild</b>	<b>Mod.</b>	<b>Sev.</b>	
<b>Events related to RMD</b>																					
Any	-	-	-	-	-	-	-	-	-	-	12	92	-	-	-	15	94	-	-	-	-
Nausea	-	-	-	-	-	-	-	-	-	-	7	54	11	3	-	10	63	14	4	-	-
Fatigue	-	-	-	-	-	-	-	-	-	-	6	46	8	2	-	8	50	11	-	-	-
Constipation	-	-	-	-	-	-	-	-	-	-	-	-	-	-	-	5	31	3	2	-	-
Headache	-	-	-	-	-	-	-	-	-	-	3	23	4	-	-	2	13	4	-	-	-
Dizziness	-	-	-	-	-	-	-	-	-	-	2	15	2	1	-	1	6	1	-	-	-
Dysgeusia	-	-	-	-	-	-	-	-	-	-	2	15	2	1	-	1	6	1	-	-	-
Abdominal pain	-	-	-	-	-	-	-	-	-	-	-	-	-	-	-	3	19	3	-	-	-
Anosmia	-	-	-	-	-	-	-	-	-	-	1	8	1	-	-	-	-	-	-	-	-
Anxiety	-	-	-	-	-	-	-	-	-	-	-	-	-	-	-	1	6	1	-	-	-
Chills	-	-	-	-	-	-	-	-	-	-	1	8	2	-	-	-	-	-	-	-	-
Hyperhidrosis	-	-	-	-	-	-	-	-	-	-	-	-	-	-	-	1	6	1	-	-	-
Injection site reaction	-	-	-	-	-	-	-	-	-	-	-	-	-	-	-	1	6	1	-	-	-
Neutropenia	-	-	-	-	-	-	-	-	-	-	-	-	-	-	-	1	6	2	-	-	-
Reflux gastroesophageal reflux disea	-	-	-	-	-	-	-	-	-	-	-	-	-	-	-	1	6	1	-	-	-
Thrombocytopeni	-	-	-	-	-	-	-	-	-	-	-	-	-	-	-	1	6	1	-	-	-
<b>Total</b>																					
	<b>Participants</b>		<b>Mild</b>	<b>Mod.</b>	<b>Sev.</b>	<b>Participants</b>		<b>Mild</b>	<b>Mod.</b>	<b>Sev.</b>	<b>Participants</b>		<b>Mild</b>	<b>Mod.</b>	<b>Sev.</b>	<b>Participants</b>		<b>Mild</b>	<b>Mod.</b>	<b>Sev.</b>	
<b>Unrelated Events</b>																					
Any	14	93	-	-	-	13	87	-	-	-	12	92	-	-	-	15	94	-	-	-	-
Sexually transmitted infection	6	40	-	11	-	3	20	-	3	-	4	31	-	5	-	5	31	-	6	-	-
Headache	3	20	2	1	-	2	13	2	-	-	1	8	2	-	-	4	25	3	1	-	-
Upper respiratory tract infection	2	13	1	1	-	1	7	2	-	-	3	23	4	-	-	4	25	2	3	-	-
Nausea	1	7	1	-	-	3	20	2	1	-	2	15	1	1	-	3	19	3	-	-	-
Fatigue	2	13	2	2	-	1	7	1	-	-	-	-	-	-	5	31	5	-	-	-	-
Skin infection	2	13	1	3	-	2	13	1	1	-	2	15	1	1	-	2	13	1	1	-	-
Constipation	3	20	3	-	-	-	-	-	-	-	2	15	2	-	-	2	13	1	1	-	-
Abdominal pain	5	33	5	-	-	1	7	1	-	-	1	8	-	1	-	-	-	-	-	-	-
Pharyngitis	2	13	2	-	-	1	7	2	-	-	1	8	1	-	-	2	13	2	-	-	-
Abdominal distension	3	20	3	-	-	-	-	-	-	-	-	-	-	-	-	2	13	2	-	-	-
Insomnia	2	13	2	-	-	1	7	-	1	-	-	-	-	-	-	2	13	1	1	-	-
Arthralgia	3	20	3	-	-	-	-	-	-	-	1	8	2	-	-	-	-	-	-	-	-
Myalgia	-	-	-	-	-	2	13	1	1	-	-	-	-	-	-	2	13	1	1	-	-
Paresthesia	1	7	1	-	-	-	-	-	-	-	1	8	1	-	-	2	13	2	-	-	-
Vasovagal reaction	-	-	-	-	-	1	7	1	-	-	2	15	2	-	-	1	6	2	-	-	-
Anxiety	1	7	1	-	-	-	-	-	-	-	1	8	1	-	-	1	6	1	-	-	-
Back pain	-	-	-	-	-	-	-	-	-	-	1	8	1	-	-	2	13	-	2	-	-
Diarrhea	2	13	2	1	-	-	-	-	-	-	1	8	-	-	-	1	6	-	1	-	-
Dyspnea	-	-	-	-	-	2	13	1	1	-	1	8	-	1	-	-	-	-	-	-	-
Eczema	-	-	-	-	-	1	7	1	-	-	-	-	-	-	-	2	13	2	-	-	-
Eye pain	-	-	-	-	-	-	-	-	-	-	-	-	-	-	-	3	19	3	-	-	-
Hyperhidrosis	-	-	-	-	-	1	7	2	-	-	1	8	1	-	-	1	6	1	-	-	-
Pruritus	1	7	1	-	-	1	7	1	-	-	-	-	-	-	-	1	6	1	-	-	-
Reflux gastroesophageal reflux disea	1	7	1	-	-	1	7	1	-	-	1	8	1	-	-	-	-	-	-	-	-
Thrush	1	7	-	1	-	-	-	-	-	-	-	-	-	-	-	2	13	-	2	-	-
Weight gain	-	-	-	-	-	-	-	-	-	-	-	-	-	-	-	2	13	2	-	-	-
Eye infection	1	7	-	1	-	1	7	1	-	-	-	-	-	-	-	-	-	-	-	-	-
Dizziness	-	-	-	-	-	2	13	2	-	-	-	-	-	-	-	-	-	-	-	-	-
Dry skin	-	-	-	-	-	-	-	-	-	-	-	-	-	-	-	2	13	1	1	-	-
Ear pain	1	7	-	1	-	1	7	1	-	-	-	-	-	-	-	-	-	-	-	-	-
Enterocolitis infectious	1	7	1	-	-	-	-	-	-	-	1	8	1	-	-	-	-	-	-	-	-
Otitis externa	1	7	-	1	-	-	-	-	-	-	-	-	-	-	-	1	6	-	1	-	-
Proctitis	1	7	1	-	-	1	7	1	-	-	-	-	-	-	-	-	-	-	-	-	-
Tinnitus	1	7	1	-	-	1	7	1	-	-	-	-	-	-	-	-	-	-	-	-	-
Alanine transaminase increased	-	-	-	-	-	-	-	-	-	-	-	-	-	-	-	1	6	-	-	-	1
Alopecia	-	-	-	-	-	1	7	1	-	-	-	-	-	-	-	-	-	-	-	-	-
Amnesia	-	-	-	-	-	-	-	-	-	-	1	8	1	-	-	-	-	-	-	-	-
Anorexia	-	-	-	-	-	-	-	-	-	-	1	8	1	-	-	-	-	-	-	-	-
Appendicitis	-	-	-	-	-	-	-	-	-	-	-	-	-	-	-	1	6	-	1	-	-
Basal cell carcinoma	-	-	-	-	-	-	-	-	-	-	-	-	-	-	-	1	6	-	1	-	-
Bloodstream infection	-	-	-	-	-	1	7	-	1	-	-	-	-	-	-	-	-	-	-	-	-
Chills	-	-	-	-	-	-	-	-	-	-	1	8	1	-	-	-	-	-	-	-	-
Cholecystitis	-	-	-	-	-	-	-	-	-	-	1	8	-	1	-	-	-	-	-	-	-
Confusion	1	7	1	-	-	-	-	-	-	-	-	-	-	-	-	-	-	-	-	-	-
Dehydration	-	-	-	-	-	1	7	1	-	-	-	-	-	-	-	-	-	-	-	-	-
Dry mouth	1	7	1	-	-	-	-	-	-	-	-	-	-	-	-	-	-	-	-	-	-
Epistaxis	-	-	-	-	-	1	7	1	-	-	-	-	-	-	-	-	-	-	-	-	-
Hypertension	-	-	-	-	-	-	-	-	-	-	-	-	-	-	-	1	6	1	-	-	-
Lung infection	-	-	-	-	-	1	7	-	1	-	-	-	-	-	-	-	-	-	-	-	-
Mental and behavioural disorder due to multiple drug use	-	-	-	-	-	-	-	-	-	-	1	8	-	1	-	-	-	-	-	-	-
Mucosal infection	-	-	-	-	-	-	-	-	-	-	-	-	-	-	-	1	6	-	1	-	-
Mucositis oral	-	-	-	-	-	-	-	-	-	-	1	8	1	-	-	-	-	-	-	-	-
Pain in extremity	-	-	-	-	-	1	7	-	1	-	-	-	-	-	-	-	-	-	-	-	-
Pregnancy	-	-	-	-	-	-	-	-	-	-	-	-	-	-	-	1	-	-	-	-	-
Radiculitis	-	-	-	-	-	-	-	-	-	-	-	-	-	-	-	-	-	-	-	-	1
Removal of mole	-	-	-	-	-	-	-	-	-	-	-	-	-	-	-	1	6	1	-	-	-